IGNEABILITY FEATURE: AN EFFECTIVE, EASY AND LOW-COST WAY TO IDENTIFY BASIC IGNEOUS ROCKS USING WIRELINE WELL LOGS IN OPEN HOLE WELLS

Filipe Vidal Cunha Santa Rosa Soares de Oliveira [1*], Ricardo Tepedino Martins Gomes [1],
Lidia Waltz Calonio [2], Krishna Milani Simões Silva [1], Isabela de Oliveira Carmo [1],
Bruno Tosta Bittencourt [1], Bruna Maia Imbuzeiro [2], Carla Semiramis Silveira [2],
Cleverson Guizan Silva [2], and Antonio Fernando Menezes Freire [2]

[1] Petrobras, Rio de Janeiro, RJ, Brazil
[2] Universidade Federal Fluminense - UFF, Niterói, RJ, Brazil

*Corresponding author email: fvidal@id.uff.br

ABSTRACT. The correct identification of igneous rocks is of fundamental importance during drilling and to the quality of the initial assessment of their role in the petroleum systems. These rocks show characteristics in geophysical well logs that are distinct from those of sedimentary rocks. After calibrating with laboratory data, we propose a method to identify and characterize igneous rocks using basic geophysical logs. This method consists of a crossover between bulk density and photoelectric factor logs to identify basic igneous rocks in sedimentary sections, named "igneability feature". This log feature consists in using the bulk density log on the scale 2.0 to 3.0 g/cm^3 in the same track as the photoelectric factor log on the inverted scale, from 12 to 2 b/e. Then, when the density log is to the right of the photoelectric factor, it denotes the presence of basic igneous rocks. Acid igneous rocks were also studied and characterized by a complementary method, which consists in a crossover between the gamma ray log and a factor calculated from the bulk density and photoelectric factor log curves. Thus, this method covers most of the varieties of igneous rock found in the Brazilian basins, such as Santos, Parnaíba and Paraná.

Keywords: igneous rocks; well logs; petrophysics; basalts; igneability feature.

INTRODUCTION

Since igneous rocks can develop several roles in the petroleum system, such as seal, reservoir, trap or heat supplier for generation (Jerram, 2015), their recognition at different scales and characterization can be strategic to the development of an oil field (Mizusaki et al., 1992; Planke, 1994; Jerram, 2015; Penna et al., 2019). In this sense, a better identification of various products of magmatic processes in petroleum basins can lead to novel ways to be applied to hydrocarbon exploration or even provide exploration in basins that were not possible until now (Thomaz-Filho et al., 2008).

In general, magmatic rocks are recorded in several onshore and offshore basins in the Brazilian margin, mostly related to the separation between South America and Africa (Thomaz-Filho et al., 2008). The most recent exploration of the Brazilian Pre-salt section in SE offshore basins hosts several occurrences of igneous rocks associated with the rifting process (Riccomini et al., 2012).

Despite the significance of volcanic rocks for oil exploration in Brazil and worldwide, the characterization of these rocks and their facies using well logs remains a challenge (Zou et al., 2013; Ran et al., 2014; Jerram, 2015; Fornero et al., 2019). The use of image logs is very useful but needs the collection of sidewall core samples (SWC) for their correct characterization during the open hole logging (Fornero et al., 2019). Some authors (Zou et al., 2013; Ran et al., 2014) point out that the characterization of these rocks should ideally be done by expensive logs such as elemental capture spectroscopy (ECS) and

resistive and acoustic image logs. However, basic well logs such as gamma ray, resistivity, sonic, density, neutron and photoelectric factor are low-cost and are a means of obtaining information regarding the faciology of these rocks when there is a limitation of samples, laboratory analyses and geophysical well logs (Nelson et al., 2009).

This work presents a proposal for the identification and differentiation of igneous rocks using basic well logs dealing with the problem of characterizing these rocks, which is usually made by rock analysis of spotted SWC samples, or demanding more complex and expensive well logs, such as imaging logs and ECS.

Igneous rocks in sedimentary basins

Volcanism is mostly associated with tectonic plate boundaries (LaFemina, 2015; Jerram et al., 2019) commonly present in sedimentary basins. It mainly presents basic composition, in the form of lava flows, or intrusive bodies, as dikes and sills (Thomaz-Filho et al., 2008). Important examples of this volcanism can be found in Mero field, as sills and subaerial lava flows (Penna et al., 2019), subaerial lava flows in the southeast of Santos Basin deepwater (Fornero et al., 2019), and volcanic basalt sequence in the south of Campos basin, characterized by pillow-lavas, pillow breccias, hyaloclastites, and laminated surge deposits (De Luca et al., 2017).

Basaltic magma is characterized by low silica concentration, low viscosity, and low dissolved gas content, when compared to more evolved acid magmas (Gill, 2010). It presents melts usually developed in effusive eruptions that can more rarely be explosive but are generally low explosive like strombolian volcanoes (Gill, 2010). These flows generate various igneous facies according to external factors, such as the fluid present at the surface (air or water), the water depth, the slope of the terrain, the viscosity of the magma, and the effusion rate (Walker, 1971; Umino, 2012).

Subaerial lava flows are formed when the magma with air creates a thin glass crust, isolating the magma below it, which is still liquid, giving origin to various morphologies, such as pahoehoe, rubbly pahoehoe and a'a (Macdonald, 1953; Walker, 1971; Self et al., 1998; Duraiswami et al., 2014). Compound pahoehoe lavas are 20 to 50 cm thick lobes, on average, composed of an outer glassy film and a crystalline interior with a vesicular or amygdaloidal structure (Macdonald, 1953). They may be

inflated due to magmatic input generating a metric morphology called sheet pahoehoes (Self et al., 1998).

The pahoehoe, rubbly pahoehoe or a'a lava morphologies, when are inflated, are characterized by a thick massive core and a vesicular top (in the case of sheet pahoehoe) or brecciated top (in the case of rubbly pahoehoe and a'a), with the a'a lavas still having breccia at the base, while the others having only small pipes (Macdonald, 1953; Walker, 1971; Duraiswami et al., 2003, 2008, 2014).

Subaqueous lava flows are characterized by rapid cooling due to the high temperature contrast of the lava in contact with water, generating very different shapes and facies from subaerial flows (Gill, 2010). This thermal shock generates volcanic glass, which is unstable and rapidly alters into palagonite, smectite and illite (Watton et al., 2013, 2014). These lava flows can also present various morphologies such as pillow, lobate and sheet lavas, which depend on the effusion rate, the viscosity of the lava and the topography (Umino, 2012; White et al., 2015).

The process for forming subqueous lava flows can also form hyaloclastites, which are originated by a nonexplosive thermal granulation in quenching processes, produced from the contact of lava with water, or during the transport down steep pillow slopes named pillow breccia (White et al., 2015). The breccias are composed of volcanic glass, igneous fragments, altered clay facies (palagonite, smectite and illite) and zeolites (Watton et al., 2013, 2014).

Pillow lavas are a type of blend of lavas, besides being the subaqueous correlate of the pahoehoe lobes (Walker, 1971), which is characterized by an abundant presence of volcanic glass on the outside of its form, vesicles (or amygdales) and radial fractures, and minute crystals and volcanic glass in its interior (Macdonald, 1953).

Subvolcanic magmatism is also common in the Brazilian sedimentary basins in the form of dikes and sills (Thomaz-Filho et al., 2008), where the dikes are tabular conduits and discordant features of the host rocks that transport the magma, and the sills are tabular subsurface compartments and concordant with the host rock that may store the magma (Marsh, 2015). Dikes and sills do not hold compositional variation, except when they are allocated with the presence of phenocrystals or when they undergo magmatic recharge during crystallization, providing in both cases fractional crystallization in the sill (Marsh, 2015).

Volcanics with composition other than the tholeiitic basalts are less common but also occur in Brazilian basins, such as acid volcanic rocks in Paraná Basin (Peate et al., 1992; Lima et al., 2012) and the alkaline ones in Espírito Santo Basin (Pires and Bongiolo, 2016; Pasqualon et al., 2019), for example. Continuous Campanian age tuff layers are also described in Campos Basin (Winter et al., 2007).

Well logs for volcanic rock identification

The identification of igneous rocks should preferably be done by ECS and imaging well logs; nevertheless, these logs are not always available from every drilled well. However, it is possible to infer the lithology using only basic well logs (Zou et al., 2013) to understand the behavior of each group of volcanic and subvolcanic rocks in terms of their compositional and morphological variations.

When it comes to the variation between basic and acid igneous rock, the acid rocks present higher gamma ray (GR) values, while the highest density (RHOB), resistivity (RES) and acoustic wave velocity (DT) values are of the basic volcanics.

These logs also decrease their values when they present brecciated facies, while GR values will increase when the igneous rock has altered facies (Zou et al., 2013; Ran et al., 2014). Hence, Millward et al. (2002) propose that some incompatible elements, such as Nb, Y, Th, U and Zr, are proportional to the content of SiO_2 in the rock and that it is possible to observe the pattern change by the values of the GR log, being Th an indicator of the chemical composition of the rock. Thus, the highest GR values are related to acid rocks but, when formed in a subaqueous environment, they are more radioactive than their underwater counterparts (Ran et al., 2014).

In subaerial lava flows, the increase of vesicles and fractures is expressed by the decrease of density, resistivity, and acoustic wave velocity, but the increase of the natural radioactivity of the rock (Planke, 1994). This natural rock radioactivity is related to the low temperature alteration of the rock, expressed by the presence of smectite and celadonite, as well as the presence of sediments between the igneous flows, while density and sonic logs respond to changes in matrix, porosity, and fluid in the pores, being affected by the alteration to clay minerals (Planke, 1994). In pillow lavas and hyaloclastite sequences, the increase in K (%) is a good indicator of the presence of clay minerals concerning to the alteration of the rocks (Brewer et al.,

1998), affecting therefore the density and sonic logs due to the presence of these altered minerals (Planke, 1994). Futhermore, it is an important indicator that can help differentiate subvolcanic from subaerial lava flows.

The subvolcanics present high values of impedance and acoustic wave velocity, and consequently higher density and lower sonic logs, when compared to the sedimentary section (Planke et al., 2005). The same characteristic in well logs is related to subaerial lava flow cores that exhibit higher density and lower sonic values, when compared to the sedimentary section, according to Bücker et al. (1998). In both cases, the caliper log shows the zones where a break-in occurs, as these are usually related to the coherent facies (Jerram et al., 2019).

DATA AND METHODS

For the development of the method presented in this study, we used public basic logs and rock data of wells from Santos, Parnaíba and Paraná basins with igneous rock occurrences (Figure 1), all provided by ANP (Brazilian National Agency of Petroleum, Natural Gas and Biofuels). These basic logs consist of gamma ray (GR), resistivity (RES), compressional sonic (DT), bulk density (RHOB), photoelectric factor (PEF) and neutron logs (NPHI).

The GR is a well log that obtains the natural radioactivity of the rock, from the elements potassium, thorium and uranium; the resistivity gives us the resistance to the passage of electric current in the rock; the sonic log reveals the transit time of the compressional wave in the formation; the neutron log indicates the porosity from a calculation of neutron absorption by the formation; the bulk density gives us a value considering the porosity as well; and the PE corresponds to an information that generates a value proportional to the average atomic number of the elements that compose the formation (Elis and Singer, 2007). The Interactive Petrophysics® version 4.6.1 software was used to analyze these well logs and generate the crossplots.

The rock data consist of lithogeochemical data (major, minor and trace elements); macroscopic description of sidewall core (SWC) and cutting samples; SWC images; X-ray diffraction (XRD); and X-ray fluorescence (XRF) data. They provided the rock mineralogical and textural characteristics, and rock classification. The mineralogy of the rock is identified by the description of the SWC or cutting samples and may be confirmed through XRD and XRF in some wells.

1	
3-PGN-5-MA	4-OGX-49-MA
3-PGN-14-MA	1-OGX-93-MA
4-PGN-11DA-MA	1-OGX-101-MA
1-OGX-110-MA	1-OGX-118-MA
1-OGX-122-MA	

2	
3-BRSA-1255-RJS	4-BRSA-1346-RJS
3-BRSA-1305A-RJS	1-BRSA-886-RJS
3-BRSA-1322-RJS	3-BRSA-1267A-RJS
3-BRSA-1343-RJ	

3	
3-BRSA-755A-RJS	8-LL-14D-RJS
7-LL-15D-RJS	7-LL-11-RJS
7-LL-28D-RJS	

4	
1-BRSA-876A-SPS	1-BRSA-1063-SPS
3-BRSA-1216DA-SPS	3-BRSA-1290-SPS
4-BRSA-971B-SPS	

5	
1-BRSA-1050-SPS	3-BRSA-957-SCS

6	
1-ELPS-4-PR	3-ELPS-7-PR
3-ELPS-8-PR	

7	
1-ES-1-RS	1-ES-2-RS
1-MC-1-RS	

8	
1-GP-1-PR	3-COST-2-PR

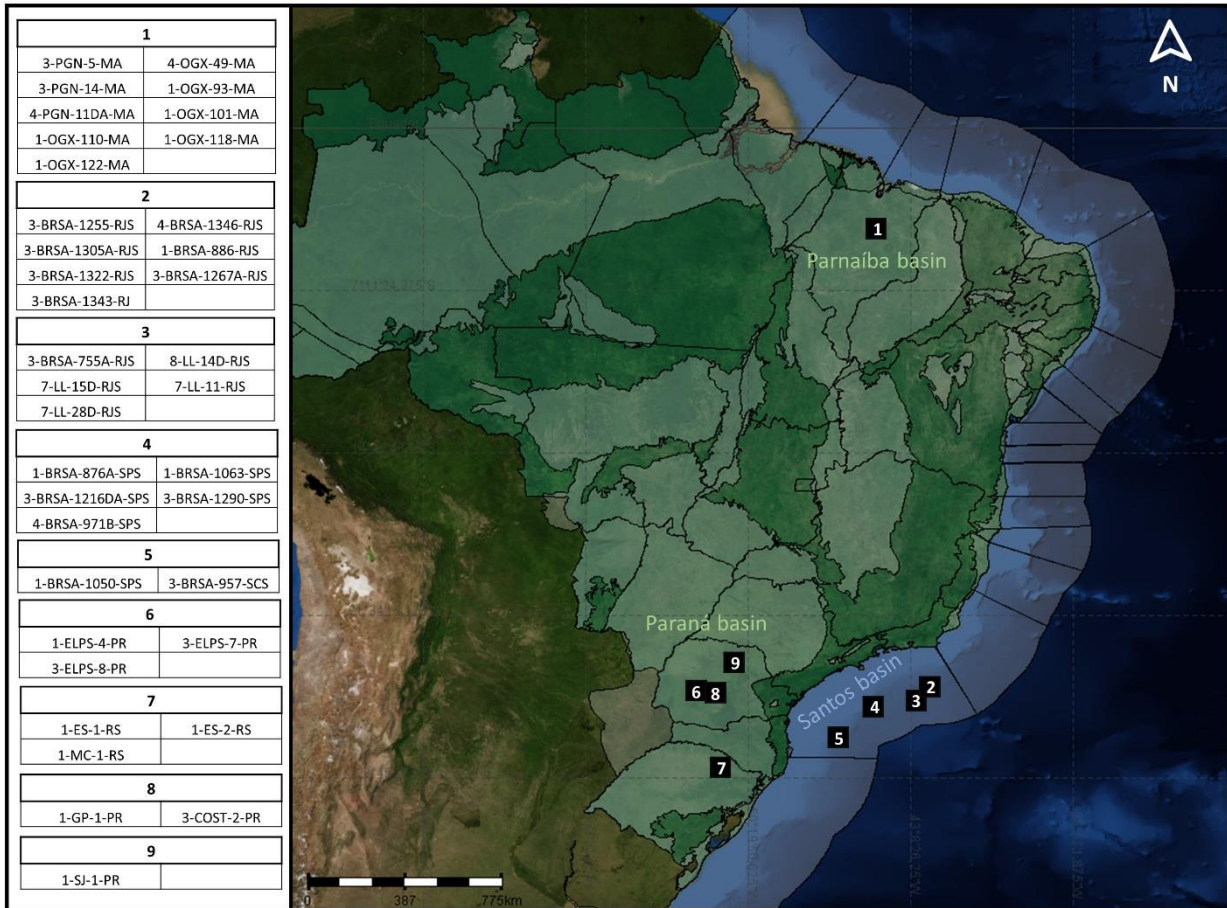| 9	
1-SJ-1-PR	

Figure 1: Location of wells in Parnaíba (1), Santos (2, 3, 4, 5) and Paraná (6, 7, 8, 9) basins. The wells in close proximity were grouped into numbered zones, as shown in the table next to the image.

The classification is obtained with geochemical data using the TAS diagram (Le Maitre et al., 2002) and is correlated with the mineralogy found in the rock, whereas the texture may be punctually described with the SWC samples. This set of basic logs and data were used together to identify igneous rocks such as basalts, diabase, rhyolites, and volcanoclastics rocks in order to recognize and understand possible false negatives and false positives from a rock-log calibration. In Santos Basin, nineteen wells were analyzed containing distinct stratigraphic igneous intervals, located in the Pre-salt, Salt and Post-salt sequences. All igneous intervals have macroscopic descriptions of sidewall core samples (SWC) and drilling cuttings, and nine wells have chemical analysis for rock classification (Table 1).

In Parnaíba Basin, nine wells from the Parque dos Gaviões gas producing field were analyzed. These wells have cuttings of diabase dikes and sills described and analyzed by x-ray diffraction (XRD) and x-ray fluorescence (XRF) (Table 1).

In Paraná Basin, nine wells with lava flows overlies the aeolian sandstones of the Botucatu Formation (Scherer, 2000; Scherer and Lavina, 2006; Scherer and Goldberg, 2007 - Table 1). Samples or rock analysis data are not available for these wells, but the type of lava flows is well characterized in the literature by the presence of bimodal subaerial lavas, chemically classified basic or acid rocks (Bellieni et al., 1984; Lima et al., 2012; Waichel et al., 2012; Rossetti et al., 2014), where the distinction of basic from acid igneous rocks was made by the technique proposed by Zou et al. (2013) and applied to all data used in this study. This author separates volcanic rocks based on two crossplots, GR x DT and GR x RHOB, grouping these rocks into four lithotypes (basalts, andesites, dacites and rhyolites), and also inferring patterns of fracture or alteration and whether they are coherent or not.

Well log features

It was observed that a crossover between the bulk density (RHOB) and the photoelectric factor (PEF)

curves can be performed to identify basic igneous rocks (basalt and diabase) in sedimentary intervals and we named this crossover as "Igneability feature" ([De Oliveira et al., 2018](#), [2019](#)). This feature represents variations on compositional and morphological characteristics and was tested in different lithologies (sandstone, siltstone, mudstone, carbonate, salt, diabase, basalts with different morphologies, rhyolite, volcanoclastic rocks and rocks that underwent contact metamorphism) to validate the method efficiency. For basalt and diabase, this log feature consists in using the density log on the scale 2.0 to 3.0 g/cm³ in the same track as the photoelectric factor log on the inverted scale, from 12 to 2 b/e. So, when there is a crossover and the density is to the right side of the photoelectric factor, a hatching is made indicating the presence of igneous mafic rock or false positives.

For comparisons of the Igneability feature with other well logs, the Ig Factor was created, which is a mathematical calculation from the Igneability (Eq. 1), measuring on a dimensionless scale the distance between the curves in order to compare the feature with other well logs, which is also a mathematical calculation that results in a value between -1 and 1 that represents the distance between both curves for a given scale. This calculation was developed from the method for calculating the DRDN ([Freire et al., 2019](#)).

From the development of this calculation, it was possible to arrive at a simplification that resulted in Eq. 1, where the Igneability factor (Ig) represents the distance between the density curves (RHOB) and the photoelectric factor (PEF), with negative values indicating basic igneous rocks (RHOB to the right of the PEF). Values close to zero indicate that both curves are overlapping, and positive values indicate sedimentary or acid igneous rock, with PEF to the right of the RHOB.

$$Ig = 3.2 - RHOB - 0.1*PEF \qquad (1)$$

On the other hand, for acid igneous rocks, a second crossover was created, called "Feature for acid igneous rocks". This was done using the gamma ray log on the 0 to 200 gAPI scale and the Ig Factor on the -2 to 2 scale, both in the same track with hatching when the GR is to the left of the Ig Factor. This crossover was also tested from several different lithologies in order to verify false positives and false negatives.

All false positives and false negatives were identified, always presenting a counterpoint to check how to know if there really is or not an igneous rock.

Rock-log calibration

Tests to understand the variations in well logs introduced in the previous topic were calibrated with cuttings or SWC samples, from which we got macroscopic description, petrophysics and geochemical analyses. These data provide an actual composition of the igneous or sedimentary rocks and help to interpret the well log response of each rock and to check the log feature or the characteristic presented.

In this direction, a total of 540 SWC samples were studied in 19 wells in Santos Basin, of which 230 have geochemical analysis. In Parnaíba Basin, the identification was done from the description, XRD and XRF analyses. On the other hand, in Paraná Basin, due to the paucity of well analyses, the available literature was used for such correlation ([Table 1](#)). Some of these wells have already been characterized by authors as to rock type or lava flow morphology ([Fornero et al., 2019](#); [Penna et al., 2019](#)). For these cases these references were used for the model calibration, as long as they are in agreement with the macroscopic or geochemical descriptions used in the present work.

RESULTS

Well logs were used to separate igneous rocks from the sedimentary ones. Then, a preliminary identification was done to previously identify if the rock is basic, intermediate or acid, based on [Ran et al. (2014)](#) and [Zou et al. (2013)](#) techniques. Knowing whether the igneous rock is intrusive or extrusive is also of high interest during the drilling of a petroleum well; so, some methods have been applied for this, such as calibrating with SWC samples and image logs to check the functionality and accuracy of the interpretations using the geophysical well logs.

Igneous Rock Classification

Igneous rocks, previously identified by well logs especially in wells of Santos Basin, have their composition confirmed by macroscopic descriptions and chemical analyses in SWC samples, from the TAS diagram ([Le Maitre et al., 2002](#)).

In Santos Basin, igneous intrusive and extrusive rocks with basic and acid compositions were analyzed ([Figure 2](#)). The acid igneous rocks studied here have rhyolitic/trachydacitic composition and are only in the wells of the Tupi field, while the basic igneous rocks have alkaline or subalkaline signature with basaltic compositions, being more common in several areas of

Table 1: Studied wells and the samples available for macroscopic description, laboratory analyses performed on these samples, and special well logs used for characterization of the igneous rocks from literature methods (Ran et al., 2014; Watton et al., 2014; Fornero et al., 2019; Jerram et al., 2019).

| Well	Basin	Rock samples	Laboratory analysis	Well log analysis
8-LL-14D-RJS	Santos Basin	SWC	-	Imaging and geochemical log
7-LL-15D-RJS	Santos Basin	SWC	Geochemical analysis	Imaging and geochemical log
7-LL-11-RJS	Santos Basin	SWC	Geochemical analysis	Imaging and geochemical log
7-LL-28D-RJS	Santos Basin	SWC	-	Imaging and geochemical log
3-BRSA-755A-RJS	Santos Basin	SWC	Geochemical analysis	-
3-BRSA-1255-RJS	Santos Basin	SWC	Geochemical analysis	Imaging and geochemical log
3-BRSA-1305A-RJS	Santos Basin	SWC	-	Imaging and geochemical log
3-BRSA-1322-RJS	Santos Basin	SWC	-	Imaging and geochemical log
3-BRSA-1343-RJS	Santos Basin	SWC	-	Imaging and geochemical log
3-BRSA-1267A-RJS	Santos Basin	SWC	Geochemical analysis	Imaging and geochemical log
4-BRSA-1346-RJS	Santos Basin	SWC	-	Imaging and geochemical log
1-BRSA-886-RJS	Santos Basin	SWC	Geochemical analysis	Imaging and geochemical log
1-BRSA-876A-SPS	Santos Basin	SWC	-	-
4-BRSA-971B-SPS	Santos Basin	SWC	Geochemical analysis	Geochemical log
1-BRSA-1050-SPS	Santos Basin	SWC	Geochemical analysis	-
1-BRSA-1063-SPS	Santos Basin	SWC	Geochemical analysis	Imaging and geochemical log
3-BRSA-1216DA-SPS	Santos Basin	SWC	-	Imaging and geochemical log
3-BRSA-1290-SPS	Santos Basin	SWC	-	Imaging log
3-BRSA-957-SCS	Santos Basin	SWC	-	Geochemical log
3-PGN-5-MA	Parnaíba Basin	Cutting	X-ray fluorescence	-
3-PGN-14-MA	Parnaíba Basin	Cutting	-	-
4-PGN-11DA-MA	Parnaíba Basin	Cutting	-	-
4-OGX-49-MA	Parnaíba Basin	Cutting	X-ray diffraction and fluorescence	-
1-OGX-93-MA	Parnaíba Basin	Cutting	-	-
1-OGX-101-MA	Parnaíba Basin	Cutting	X-ray diffraction and fluorescence	-
1-OGX-110-MA	Parnaíba Basin	Cutting	X-ray diffraction and fluorescence	-
1-OGX-118-MA	Parnaíba Basin	Cutting	-	-
1-OGX-122-MA	Parnaíba Basin	Cutting	-	-
1-ELPS-4-PR	Paraná Basin	-	-	-
3-ELPS-7-PR	Paraná Basin	-	-	-
3-ELPS-8-PR	Paraná Basin	-	-	-
1-ES-1-RS	Paraná Basin	-	-	-
1-ES-2-RS	Paraná Basin	-	-	-
1-MC-1-RS	Paraná Basin	-	-	-
1-GP-1-PR	Paraná Basin	-	-	-
3-COST-2-PR	Paraná Basin	-	-	-
1-SJ-1-PR	Paraná Basin	-	-	-
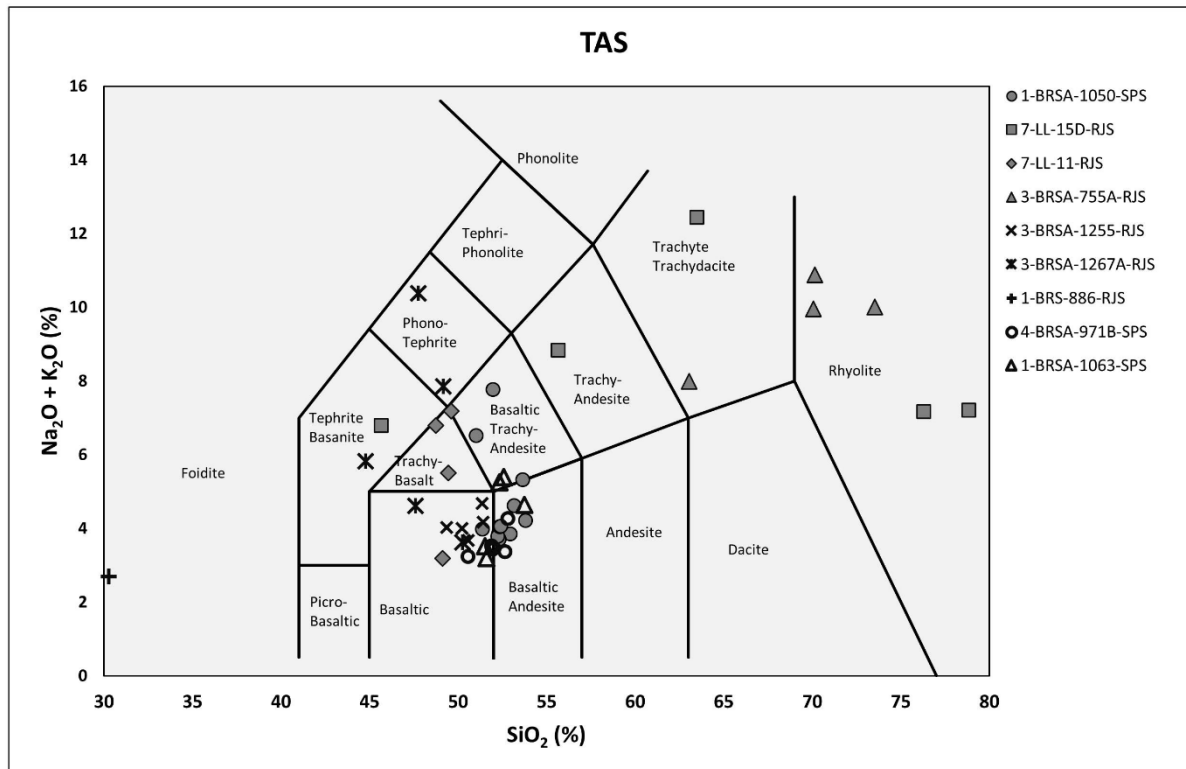
Figure 2: Classification chart of igneous rocks (TAS - Le Maitre et al., 2002) by chemical analyzes of SWC from some wells studied in Santos Basin.

the basin as intrusions and extrusions (Figure 2). In these wells, the SWC samples identified mainly carbonates in the Pre-salt section as host rock, or halite and anhydrite of the Ariri Formation as diabase intrusion.

In Parnaíba Basin, nine wells were analyzed at Parque dos Gaviões, a gas-producing area. These wells have intrusions associated with the Mosquito and Sardinha Formations, both in the form of diabase intrusions (De Miranda et al., 2018). The X-ray diffraction analysis of the igneous rocks in these wells predominantly shows plagioclase and pyroxene composition (Figure 3). In these wells the host rocks are shales, sandstones, or black shales, identified by description of cuttings and characterization by well logs and X-ray diffraction.

In Paraná Basin, 9 wells were studied in order to test the method in a known basin. However, these wells do not present SWC sample analysis, so the identification of these volcanic rocks was done by cuttings and the Zou et al. (2013) method to distinguish acid from basic igneous by well logs (Figure 4). The host rocks were identified as sandstones and shales mainly from the description of cuttings and characterization by well logs.

Igneability feature

We propose the "Igneability feature", a technique that uses bulk density (RHOB) and photoelectric factor (PEF) logs as a crossover that separates basic igneous rocks from sedimentary ones, due to the difference between both lithological types in relation to the bulk density of these rocks and the atomic number of the elements that compose the mineralogy. Meanwhile, the drilling environment is complex and there is a need to identify situations in which the crossover will suggest the presence of igneous rocks, even if they are not, or the opposite. However, it is worth noting that exceptions are occasional and how to distinguish false positives and false negatives will be discussed.

As the mineralogy of a mafic igneous rock is quite different from the one of sedimentary rocks, the bulk density and photoelectric factor logs vary considerably from the ones of the sedimentary rocks. However, acid igneous rocks have a mineralogy very similar to the siliciclastic sedimentary rocks, both being mainly composed of quartz, alkali feldspars and sodium plagioclase. This makes it difficult to separate both using these two geophysical well logs.
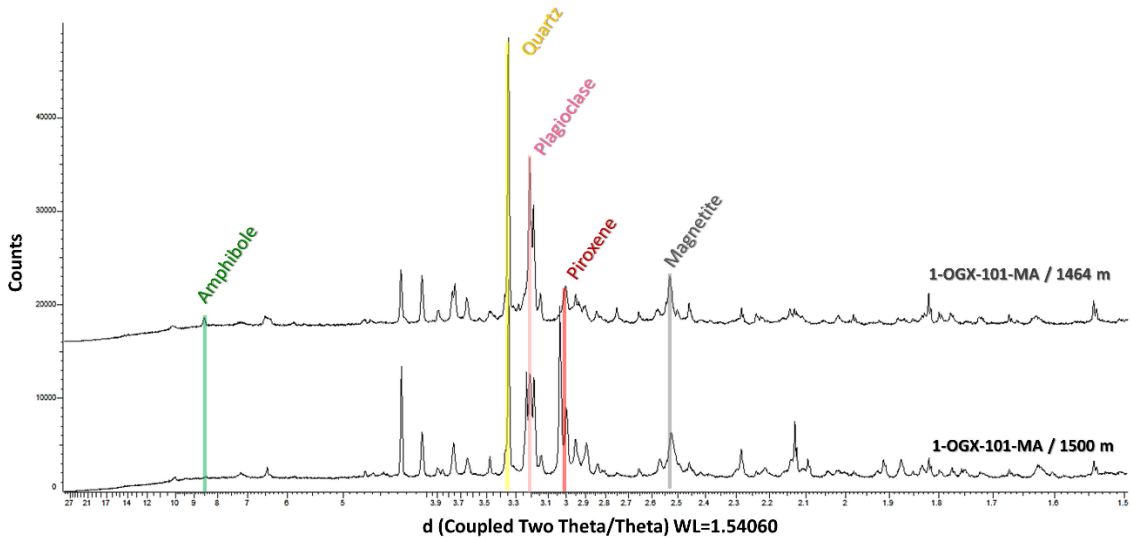
Figure 3: Result of two X-ray diffraction analyses, carried out on drill cutting samples from igneous rocks in well 1-OGX-101-MA in Parnaíba Basin, proving the main composition of the lithology as pyroxene, plagioclase, quartz, amphibole, and magnetite. The presence of quartz is ambiguous due to the possibility of this solid material being in the drilling fluid or related to the enclosing sandstone.
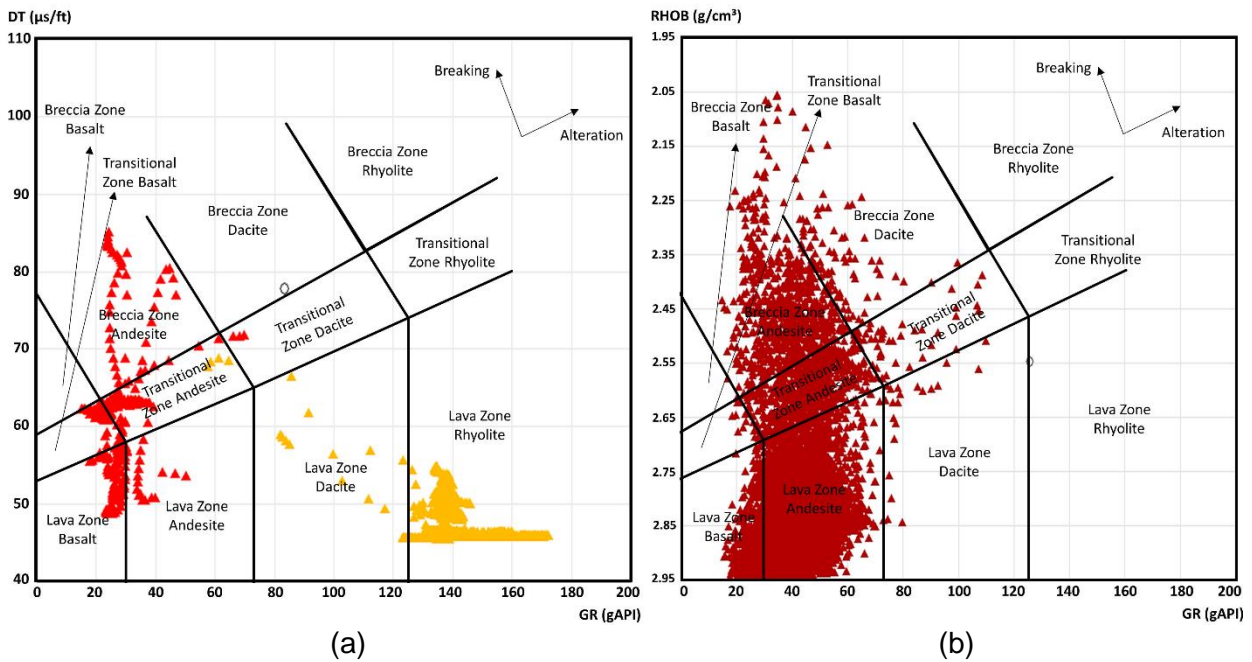

Figure 4: Two crossplots modified by Zou et al. (2013), a) one being the relationship between gamma rays and sonic logs of basic and acid composition intrusions in Paraná Basin and b) the other between gamma rays and density bulk of a sequence of basic lava flows of Serra Geral Fm. in Paraná Basin.

Contrast between basic igneous and sedimentary rocks

In Parnaíba and Paraná Basins, it is common to have intrusions into siliciclastic sedimentary sequences composed of sandstone, siltstone, and shale. These sedimentary lithologies present a pronounced contrast between RHOB and PEF when compared to igneous rocks; so, the Igneability feature works well in these situations, as the example from well 1-OGX-110-MA (Figure 5a), with three diabase intrusions, composed by plagioclase, pyroxene, and olivine, characterized by XRD on cuttings, showing a mineralogy composed of plagioclase, pyroxene, and olivine (De Oliveira et al. 2021; Imbuzeiro, 2021). These intrusions present a well-defined crossover for host rocks like mudstones, silts, and sandstones in this basin. This pattern is repeated in the
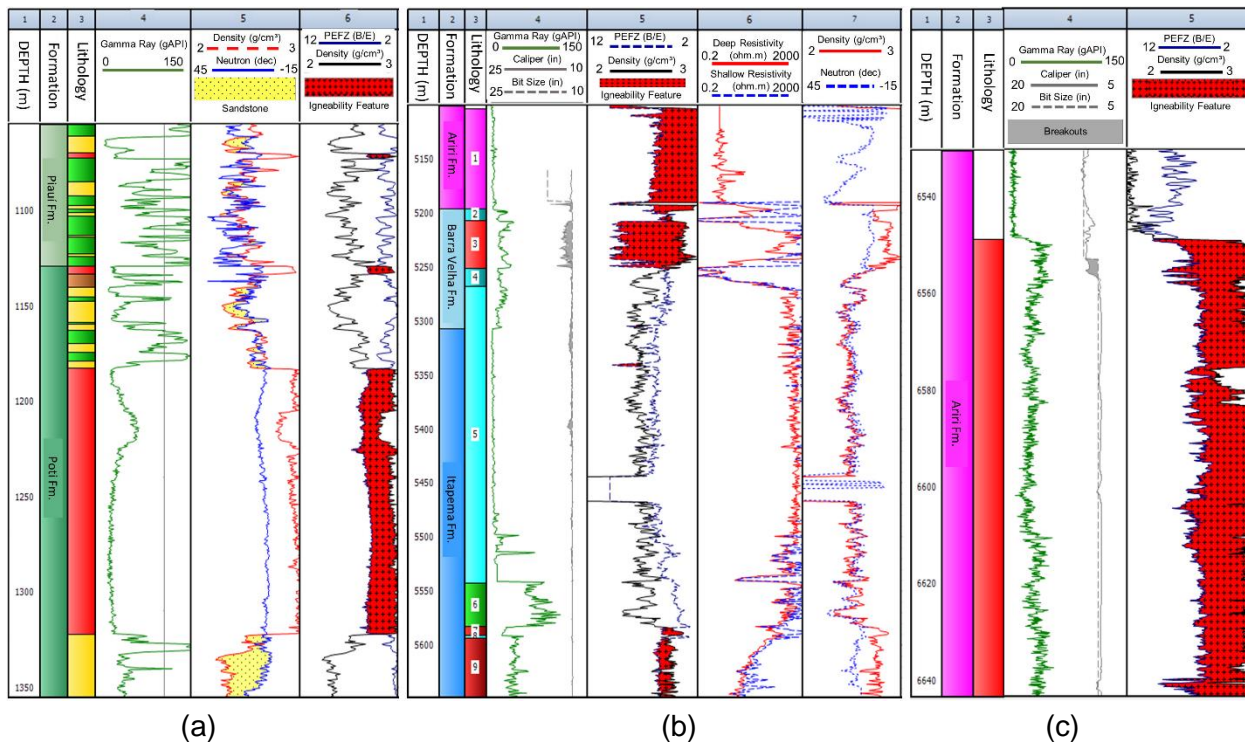
Figure 5: Three wells presenting different cases with the Igneability feature: a) Well 1-OGX-110-MA in Parnaíba Basin showing some diabase intervals (red in track 3) intruded in sandstones (yellow in track 3), siltstones (brown in track 3) and shales (green in track 3); b) Well 3-BRSA-1255-RJS in Santos Basin showing Pre-salt carbonates (light blue in track 3) below an anhydrite layer (pink in track 3) with two associated igneous layers: a diabase intrusion (red in track 3) in carbonate rocks (dark blue in track 3) and basalts (dark red in track 3). The anhydrite forms a false negative in the Igneability feature; c) Well 1-BRSA-876A-SPS in Santos Basin showing the contact between a diabase (red in track 3) and the halite of Ariri Fm. (white in track 3).

other wells in this basin as well as in Paraná Basin, with intrusions in different stratigraphic positions.

When the intrusions occur in carbonates of the Santos Basin Pre-salt, as in well 3-BRSA-1255-RJS (Figure 5b), the crossover also occurs in the igneous rock, but forms a transitional contact near the most proximal portion of the carbonate that may have undergone a thermal effect, with the PEF and RHOB coming closer together, but still with the RHOB to the right, according to the expected response for an igneous rock (Figure 6b). In the basal portion of this well, there is another igneous rock interval, a subaqueous extrusive basalt (Penna et al., 2019), but does not display zones under thermal effect; then the crossover can be seen without the transitional portion, working, in turn, as a sign of intrusive or extrusive magmatism. The entire lithological interpretation of this well was adjusted with description and analysis in a SWC sample, as described by Penna et al. (2019). These characteristics described above, referring to igneous rocks in carbonate sequences, are repeated in several wells in the Pre-Salt, including the exploratory wells and in the Mero and Tupi fields.

Some intrusions can occur in the saline section in wells of Santos Basin, as in the example of well 1-BRSA-876A-SPS (Figure 5c). In this well a diabase intrusion was identified in the halite of the Ariri Fm., where the crossover was formed without any transition referring to possible thermal effect. Descriptions of the SWC samples showed a diabase with fine phaneritic texture and plagioclase phenocrysts.

Diabases and host rock log features

The intrusive basic igneous rocks (diabase) are totally massive and therefore do not present great variation in the bulk density log; thus, the Igneability feature is very homogeneous and with high separation between the RHOB and PEF curves (Figure 5b). Besides having their GR values varying between 20 and 50 API, they have high resistivity values, low sonic ones, and the density with high values and always to the right of the neutron. Commonly, these rocks have a caliper indicating breakout (Jerram et al., 2019), due being massive and presenting a natural fracturing pattern because of the cooling process (Figure 6b).
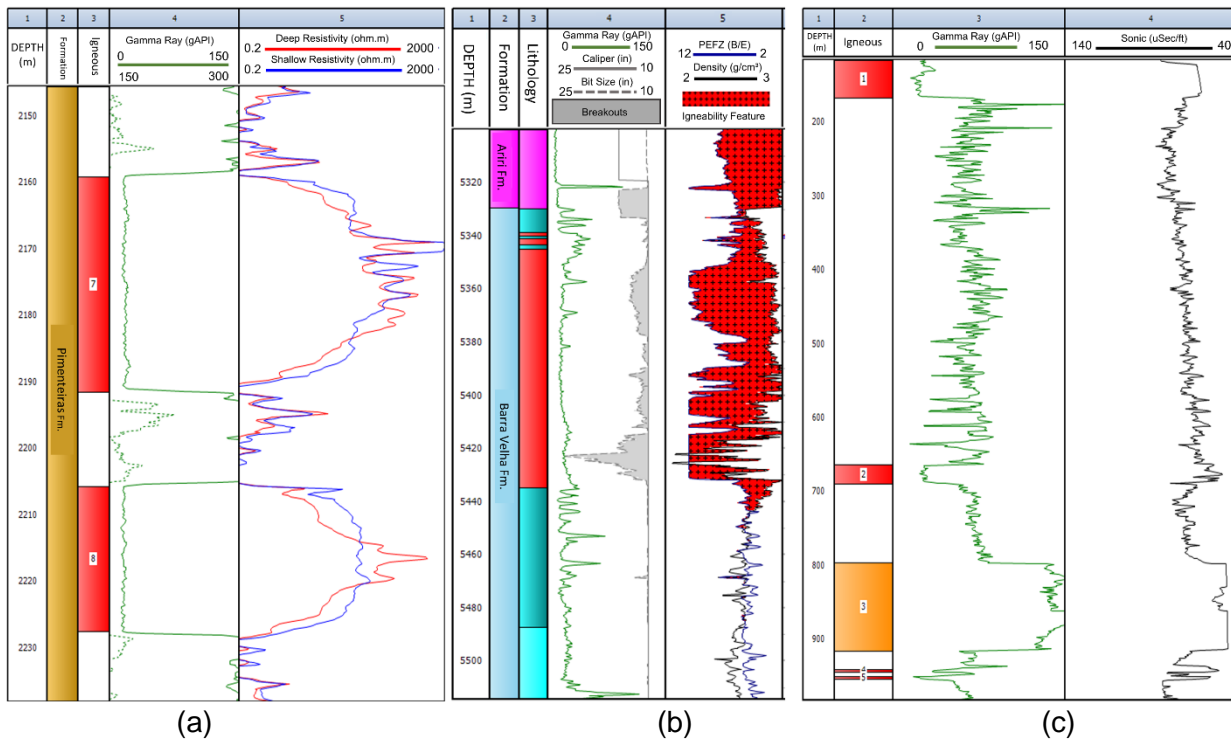
Figure 6: Three wells presenting different cases with the Igneability feature: a) Well 1-OGX-93-MA in Parnaíba Basin showing some diabase intervals (red in track 3) intruded into generator shales (white in track 3) of Pimenteiras Fm.; b) Well 3-BRSA-1305A-RJS in Santos Basin showing a diabase (red in track 3) intruded into Pre-salt carbonates (light blue in track 3) forming a contact metamorphic zone noticeable in well logs (dark blue in track 3), above all anhydrite (pink in track 3); c) Well 1-SJ-1-PR in Paraná Basin showing diabase sills (1 and 2 in red in track 3) and rhyolite (3 in orange in track 3) in an undifferentiated sedimentary section (white in track 3), in addition to possible diabase dykes (4 and 5 in red in track 3).

An igneous intrusion affects the host rocks in different ways, depending on the sedimentary rock. Three examples of intrusions into distinct sedimentary rocks show different relationships with the Igneability feature (Figure 5). The relation of intrusion and siliciclastic sedimentary host rock reveals that the Igneability feature decreases the crossover at the exact contact between the igneous and the sedimentary lithologies, but the distance between the PEF and RHOB logs is somewhat smaller in the sandstone or shale affected by the intrusion. This is not observed in sandstones and shales that have suffered little influence from the intrusion. If such intrusion occurs in an immature shale (Figure 6a), the heat will cause oil and gas generation (Dos Anjos and Guimarães, 2008), exhibiting in the portion most proximal to the igneous rock a zone with very low resistivity called Contact Low Resistivity Zones (CLRsZ), according to Spacapan et al. (2020).

This process occurs also in well 1-OGX-93-MA where the CLRsZ occurs due to several intrusions in the Pimenteiras Fm., presenting apparent thickness of up to half of the thickness of the diabase sill (Figure 6a). Intrusions in carbonate sequences, which occur in the

Santos Basin Pre-salt, can also present this CLRsZ when this carbonate is an oil reservoir (Figure 5b). This thermal contact zone causes a transitional effect on the Igneability feature, causing the crossover not to break up exactly at the contact between the igneous and the carbonate rocks, but at a certain distance, that varies from intrusion to intrusion, but always less thick than the CLRsZ, when it is present, as we can observe in Figures 5b and 6b.

Intrusions in saline sequences, with halite as host rocks, have little effect on the Igneability feature, with the occurrence of only a thin zone (just under 5 m for an intrusion of 280 m in 1-BRSA-876A-SPS), where the RHOB and PEF logs are very close to each other, but without developing the crossover (Figure 5c).

The identification of false positives when using the Igneability feature is very important to understand these limitations and to know how to work around them (Table 2). The clearest situation is the presence of anhydrite in the sedimentary section, since it presents RHOB and PEF logs like diabase intrusions, as we can see in Santos (Figures 5b and 6b) and in Parnaíba Basins (Figure 7a). Other false positives are related to

Table 2: Relationship between false positives and false negatives in the Igneability feature for each rock and how to identify them. *Breakout zone applies to any rock.

Rock	Method exceptions	Example of occurence	Criteria to determine
Carbonatic host rocks	False positive	Figure 6b	Carbonate near an intrusive igneous rock. DRDN $\cong$ 0
Anhydrite	False positive	Figures 5b, 6b and 7a	GR $\leq$ 10 gAPI; NPHI $\leq$ 0%. Homogeneous well log patterns.
Dolomites or crystalline limestones	False positive	Figure 7a	The RHOB and NPHI are close or together, DRDN $\cong$ 0. RHOB $\leq$ 2.84 g/cm³.
Breakout zone*	False positive	Figure 7b	Caliper log >> bit size, PEF increases and RHOB decreases.
Hialoclastites	False negative	Figure 8a	0.1 < DRDN < 0.5 (distance between RHOB and NPHI similar to massive basalt); 10 < GR < 90 gAPI; 1 < RES < 20 Ωm
Autobreccia	False negative	Figures 8b and 8c	0.1 < DRDN < 0.5 (distance between RHOB and NPHI similar to massive basalt); 30 < GR < 90 gAPI; 1 < RES < 40 Ωm
Vesicular or amygdaloidal basalt	False negative	Figures 8b and 8c	0.1 < DRDN < 0.5 (distance between RHOB and NPHI similar to massive basalt); 30 < GR < 50 gAPI; 1 < RES < 40 Ωm
High altered basalt	False negative	-	Depending on the degree and type of alteration of the basalt, the relationship between RHOB and NPHI changes little, just getting closer than the one for a massive basalt. However, a high alteration may prevent this technique from identifying it as basalt, requiring laboratory analysis.
Acid igneous rocks	False negative	Figures 12a and 12b	Use the Igneability feature for acid igneous rock.

carbonate host rocks (Figures 5b and 6b), dolomites or crystalline limestones (Figure 7a), some metamorphic rocks and breakout zones. They are summarized in Table 2 and will be detailed in the topic Discussion.

Basalt log features

The extrusive igneous basic rocks (basalts) can be divided into two groups: subaqueous and subaerial lava flows. Both present morphologies that control the structure and the presence of volcanic glass or alteration minerals and both present patterns in the Igneability feature that are different from the diabase ones and are distinct from each other.

The subaqueous outcrops are mainly composed of pillow lavas and hyaloclastites, where the Igneability feature works well, with the exception of some hyaloclastites with much alteration to clay minerals,

causing the curves to come close and even uncross the crossover in some cases. The average distance between RHOB and PEF in the crossover will be up to twice smaller than in the diabase and will present a more irregular behavior in the well logs (Figure 8a).

Subaerial lava flows are composed of a succession of various morphologies such as pahoehoe, rubbly pahoehoe and a'a. Some of these morphologies may have a massive core (sheet pahoehoe, rubbly pahoehoe and a'a), but normally associated with a vesiculated or brecciated facies at the top or top and bottom (Macdonald, 1953; Walker, 1971; Duraiswami et al., 2003, 2008, 2014). The vesiculated and brecciated facies provide a drop in the RHOB curve at the top of the sheet pahoehoe and the rubbly pahoehoe (Nelson et al., 2009), then they may not provide the crossover of the Igneability feature depending on the percentage of vesicles and the degree of breccia
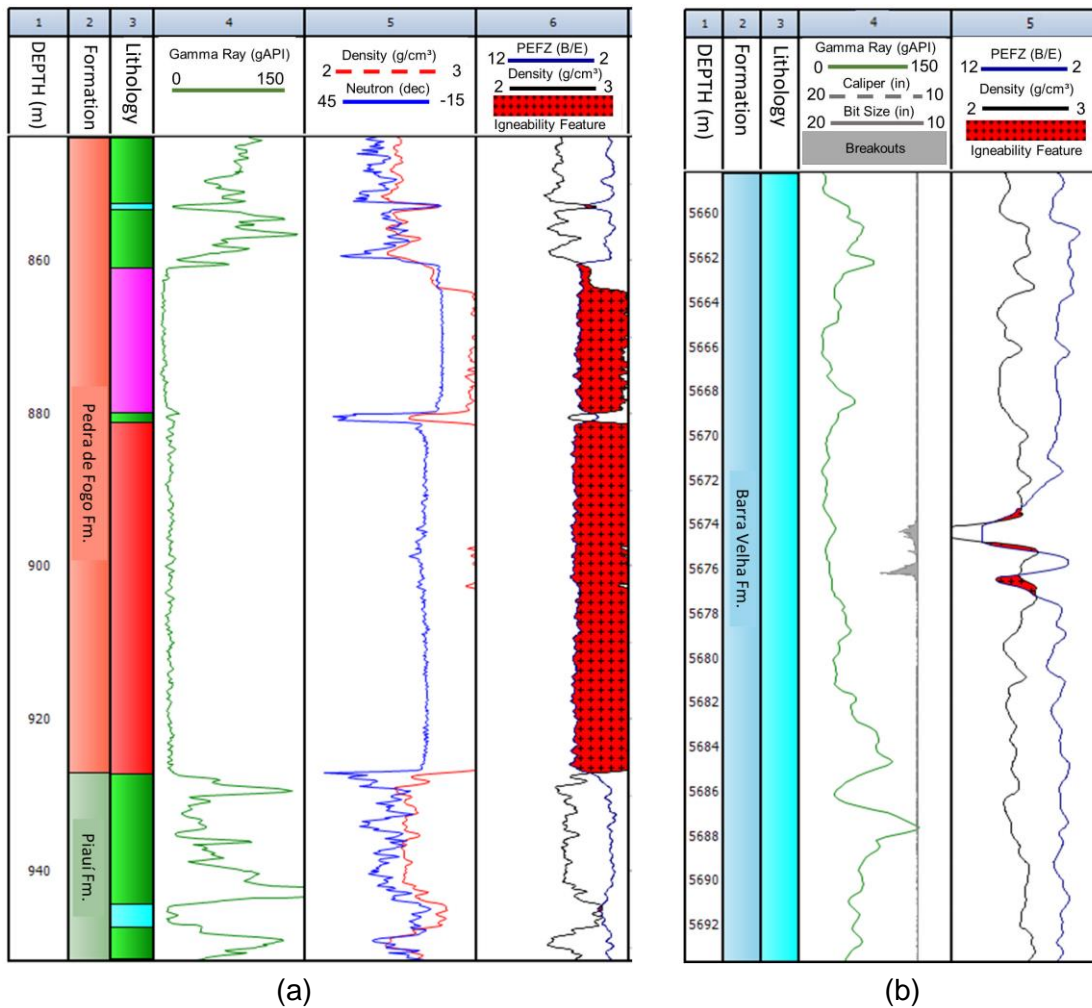
Figure 7: Two wells showing different cases with the Igneability feature: a) Well 1-OGX-110-MA in Parnaíba Basin showing some diabase (red in track 3) intruded into a sedimentary section composed of shales (green in track 3), carbonates (blue in track 3) and anhydrite (pink in track 3); b) Well 3-BRSA-1305A-RJS in Santos Basin showing Pre-salt carbonates (light blue in track 3) with a breakout zone evidenced by the caliper log.

compaction. For this reason, the subaerial flow sections show an intermittent pattern (crossover and not crossover) in the igneability feature where it is possible to observe that every flow has a crossover at the base and does not have one at the top (Figures 8b and 8c).

Igneability Factor (Ig): a comparison with other well logs

The integrated use of the Ig factor with the other well logs allows us to study and understand geological variations such as the composition of the igneous rock (basic or acid), their facies (massive, vesicular or brecciated) or the degree of alteration (due to the presence of glass). When we compare it with the GR log it is possible to see the correlation cited by Ran et al. (2014), where more acid igneous rocks have higher GR values, and compare this with our observations about the fact that the Igneability feature does not see the acid igneous rocks. In this sense, the same reasoning can be applied for the basic

igneous rocks (Figure 9a), where lower GR values are observed and a comparison with the Ig factor is also possible. However, there are facies variations that are best observed in basic volcanics and actual variations as to the response of the Igneability feature.

Low resistivity volcanic facies are directly related to Ig values close to zero and even positive; these facies are related to vesiculate zones or breccias in subaerial flows (Nelson et al., 2009). Subaqueous facies may also show lower resistivities depending on the volcanic glass content formed (Watton et al., 2013, 2014). These same relationships between Ig and resistivity are observed with compressional sonic, relating Ig near zero to high transit times (Figure 9b).

Comparing the clay porosity of the Nuclear Magnetic Resonance log (NMR) with the Ig factor, it can be seen that the presence of clay is related to Ig values close to zero or positive. This means that alteration becomes the factor that most affects the
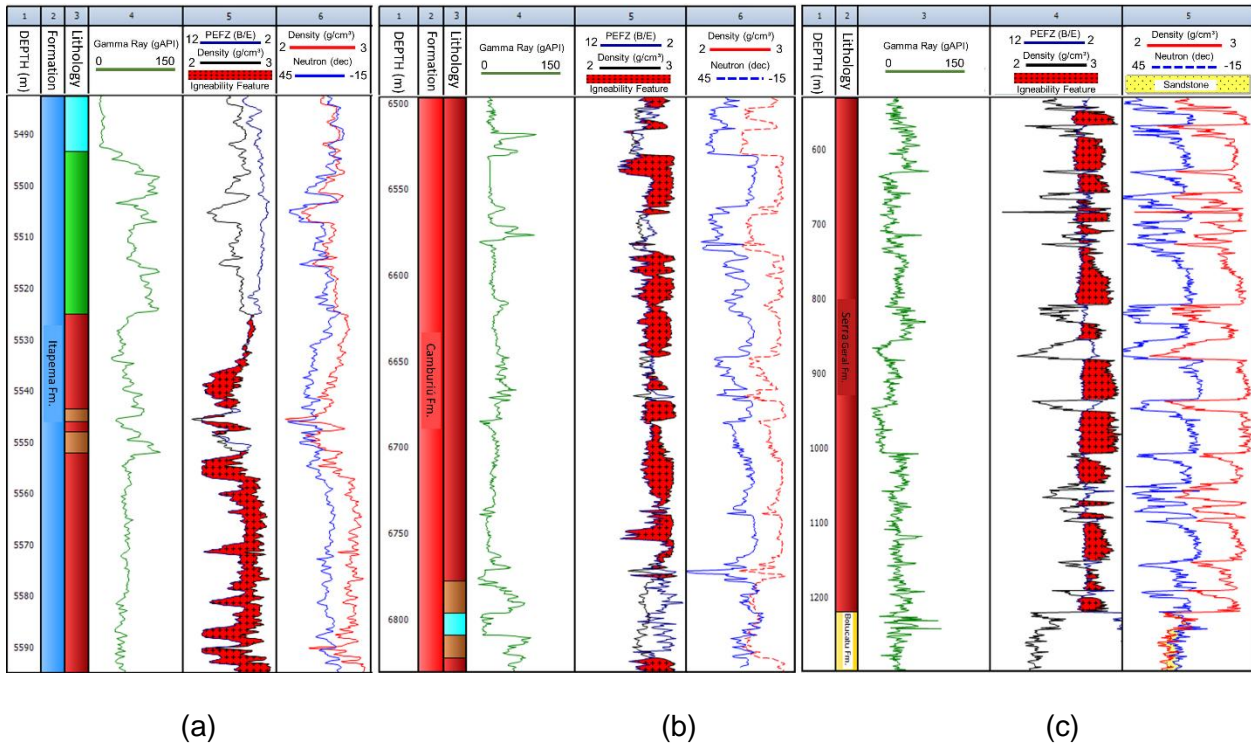
Figure 8: Three wells presenting different cases with the Igneability feature: a) Well 3-BRSA-1343-RJS in Santos Basin showing basalts (reddish brown in track 3) interspersed with siltstones (brown in track 3), both below carbonates (blue in track 3) and shales (green in track 3); b) Well 3-BRSA-1050-SPS in Santos Basin showing subaerial basalts (according to Fornero et al., 2019) (reddish brown in track 3) intercalated with siltstone (brown in track 3) and carbonate (blue in track 3); c) 3-ELPS-8-PR well in Paraná Basin showing basalts (reddish brown in track 3) from Serra Geral Fm. on the aeolian sandstones (yellow in track 3) of Botucatu Fm.
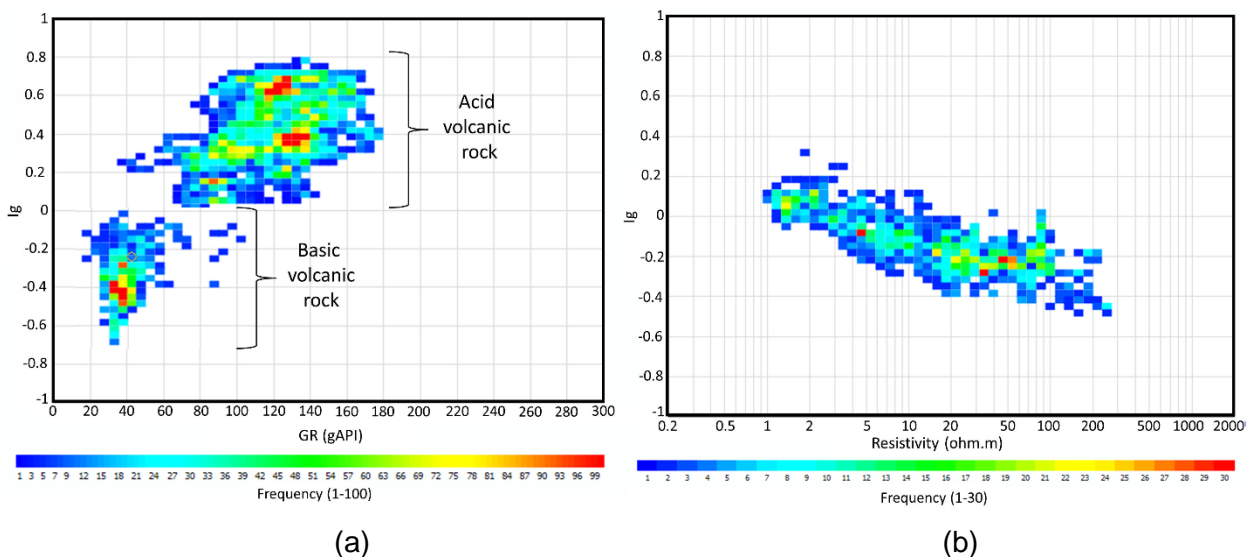
Figure 9: Two-point frequency crossplots showing the standard behavior of acidic and basic igneous rocks: a) Gamma ray and Ig crossplot indicating specific zones for the two types of volcanic rocks; b) Resistivity and Ig crossplot showing a trend of Ig variation as a function of resistivity in basic igneous rocks. The colors of the dots indicate frequency.

Igneability feature in basic igneous rocks, as this correlation also works for low resistivities and high transit time, all common characteristics of the presence of clay minerals (Figure 10).

The values in GR increase proportionally with the variation of acidity of the igneous rock because acid igneous rocks have minerals enriched in K and Th, which provide higher values of GR (Ran et al., 2014). Meanwhile, it is also possible to make the correlation of the increase of the igneous rock acidity with the decrease of density, because the basic and ultrabasic rocks tend to be denser than the intermediate and acid ones, due to the density of the essential minerals that compose them, as olivine and pyroxene which are denser than feldspar and quartz (Ran et al., 2014). As the PEF is also proportional to the matrix density of the rock (Ellis and Singer, 2007), there is a tendency for the Igneability feature not to appear in intermediate and mainly acid igneous rocks (when we ignore facies variations and only consider massive rocks). The relationship between Ig vs. GR and Ig vs. Resistivity indicates this trend and infers the response of the intermediate and ultrabasic igneous rock. The same is noted when using crossplots Ig vs. Sonic and Ig vs. NMR log (Figure 10).

The relationship between RHOB and NPHI logs indicates the composition of the igneous rock present in the well. The acid rocks present variations that are confused with sandstones and shales, because the spacing of these logs are directly related to the mineralogical composition. The crossplot NPHI x RHOB shows well the relationship between both of them, where the acid rocks are in the same trend of the porosity variation of sandstones and the basic igneous rocks have a different trend but starting from denser compositions below the trend of the porosity variation of the dolomite (Figure 11a). The trends of intermediate and ultrabasic rocks can be inferred from the expected matrix density for such a composition since we did not have these examples in the study.

To understand how this variation in RHOB and NPHI responds to variation in the Igneability feature, we compare the Ig with the DRDN (Freire et al., 2019). Thus, it is possible to observe that as the DRDN becomes negative (density to the left of neutron), the Ig becomes positive (density to the left of PEF), forming a trend of compositional variation (considering massive facies) that allows confirming that the working edge of the Igneability feature is in the intermediate rock (Figure 12b). Thus, based on this composition, the GR becomes the best parameter for correct lithological identification.

Based on the GR, RES, Ig and DRDN log patterns of acid igneous rocks (extrusive and intrusive), mafic intrusions (diabases), mafic basaltic lava flows (subaerial and subaqueous), the Table 3 presents a summary of the differences between between the rocks and the facies that do not show the crossover of the Igneability feature.

Igneability feature for acid igneous rock

Due to the fact that acid igneous rocks have high GR values, regardless of whether they are coherent or volcanoclastic, we associate the Igneability factor calculated from the Igneability feature with the GR log, where the Ig varies with scale from -2 to 2 and the GR varies with scale from 0 to 200 gAPI. Thus, we observed that:

- zones with basic rocks present the GR to the left of the Ig and the Ig with values below zero;
- when the Ig has values above zero and the GR remains to the left, the rock is sedimentary;
- when the GR is to the right of the Ig (always above zero), it is an indication of acid igneous rock (track 5 in Figures 12a and 12b).

The acid igneous rocks are characterized by high values of GR, but, when their facies are volcanoclastic and have low resistivity and low bulk density logs (Ran et al, 2014), they show values closer to sedimentary rocks such as sandstones and shales. Rhyolites exhibit a relationship between RHOB and NPHI curves similar to sandstones, even when they are volcanoclastic. However, the sandstones do not show such high values of GR, which in rhyolites easily reach 150 gAPI.

Shales are the only sedimentary rocks that can reach high radioactivity as a rhyolite can, but only when they have high organic matter content. Nevertheless, shales have a ratio between RHOB and NPHI that is inverse to that expected for rhyolites. Therefore, it is possible to distinguish these cases from false positives.

Some acid igneous rocks with a trachydacitic composition are somewhat less radioactive and have the ratio of RHOB and NPHI similar to that of a carbonate, but the set of well logs allows us to distinguish them from shale, sandstone and carbonate.

Some very altered zones in basic igneous rocks can reach high GR values and fit as exceptions regarding the Igneability feature, that is, it is a basic igneous rock, but the Igneability feature does not crossover. When the degree of alteration is very high, such as some rare
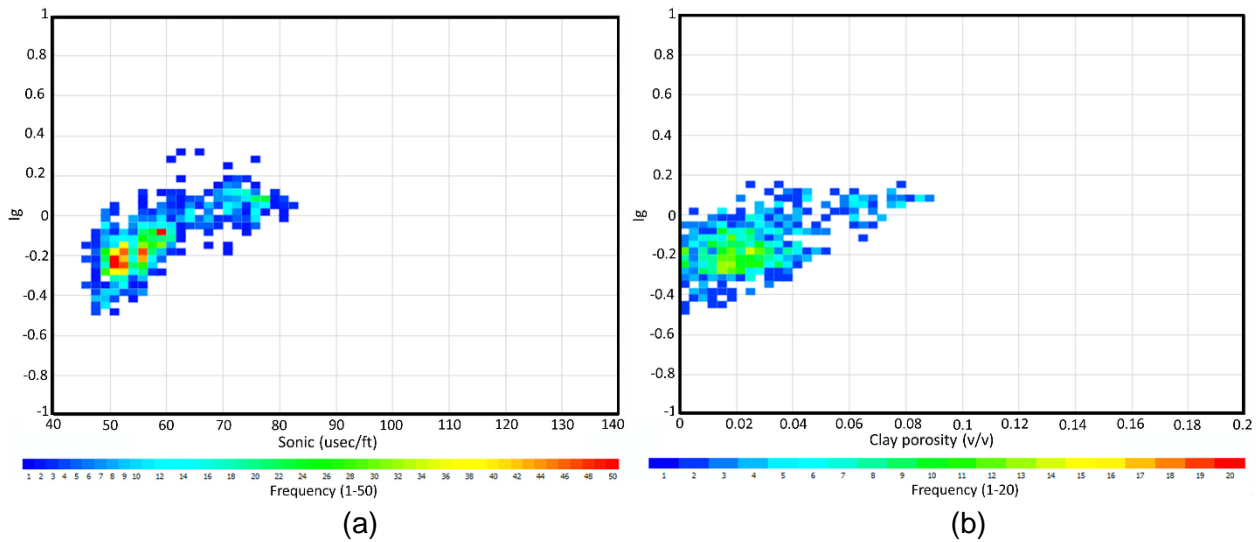
Figure 10: Two-point frequency crossplots relating the Ig to other well logs in basic igneous rocks: a) Ig related to Sonic, indicating a variation trend between them; b) Ig related to the NMR clay porosity, also indicating a trend between them.
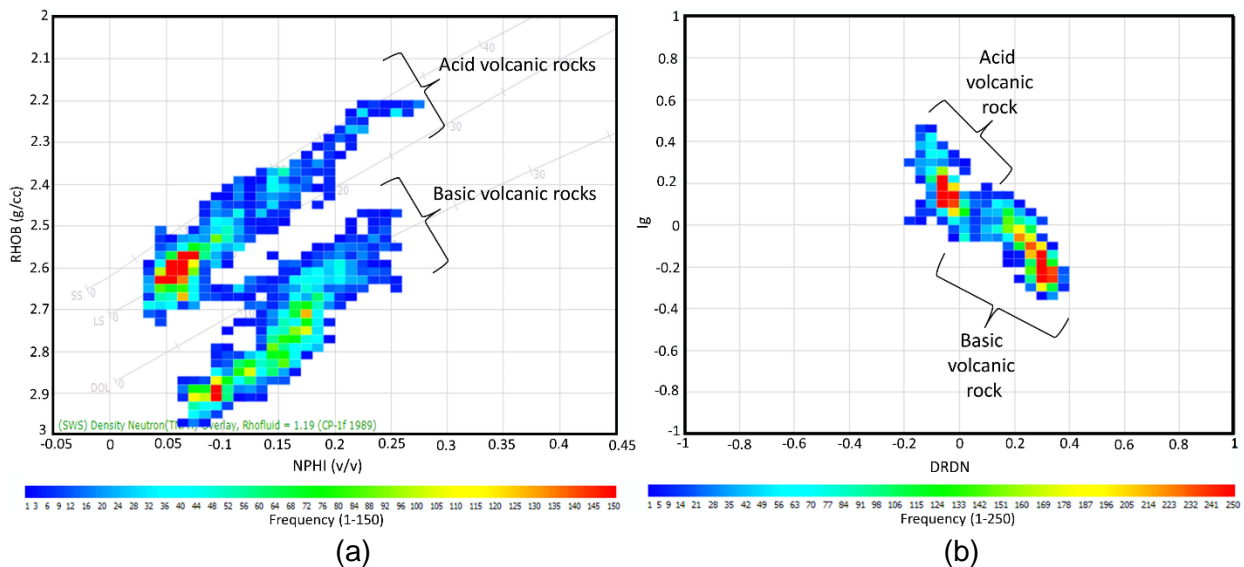

Figure 11: Two point frequency crossplots, where the red dots indicate a higher concentration of the points and the blue ones indicate a lower concentration: a) Crossplot RHOB vs. NPHI showing the porosity variation lines of sandstone, limestone and dolomite, with two distinct point clouds, the upper one related to the acid volcanics and the lower one related to the basic volcanic rocks; b) Crossplot DRDN (calculated according to Freire et al., 2019) by Ig showing that acid volcanics have positive Ig and a density and neutron variation similar to a sandstone, while basic volcanic ones have negative Ig and DRDN positive, similar to shales.

cases in hyaloclastites or rubbly top breccias, the GR may form a crossover with the Ig indicating a rhyolite, but usually this is very occasional and the RHOB and NPHI relationships remain as a basalt.

DISCUSSION

From the results and direct interpretations, it is possible to reach some discussions about the false positives and negatives in the Igneability feature, lava morphology, and the composition and texture of the rock from the geophysical well logs of petroleum wells. These interpretations can be made with different degrees of certainty depending on the available well logs and the degree of alteration of the rock.

False positives in sedimentary basins

The anhydrite is the main false positive in the igneability method. However, the anhydrite has extremely low

Table 3: Relation between the types of igneous rocks presented in this work and how to identify them from the Igneability feature, DRDN, GR and RES, as well as the figures with examples of each.

Igneous rock	Method exceptions	Example of occurence	Criteria to determine
Diabase	no	Figures 5a, 5b, 5c, 6a, 6b, 6c and 7a	Well logs normally linear and without zones of low resistivity or density. 15<GR<50 API; 50<RES<2000 Ωm; -0.8<Ig<-0.1
Subaerial basalt	On highly vesiculated facies or breccias	Figures 8b and 8c	Well logs of interspersing zones of high and low resistivity and density. 15<GR<100 API; 1<RES<1000 Ωm; -0.6<Ig<0.2
Subaqueous basalt	On glassy-rich facies (clay or palagonite), mainly breccias	Figures 5b, 8a and 12a	Well logs tend to have lower resistivity and density values; in the exceptions there may be shallow resistivity values greater than the deep resistivity one. 20<GR<90 API; 1<RES<1000 Ωm; -0.6<Ig<0.2
Riolite or Dacite	All facies	Figures 12a and 12b	Very high GR log, with resistivity and density varying according to facies. The igneability feature for acid igneous rocks should be used (crossover between Ig and GR). 110<GR<230 API; 1<RES<1000 Ωm; 0.1<Ig<0.8
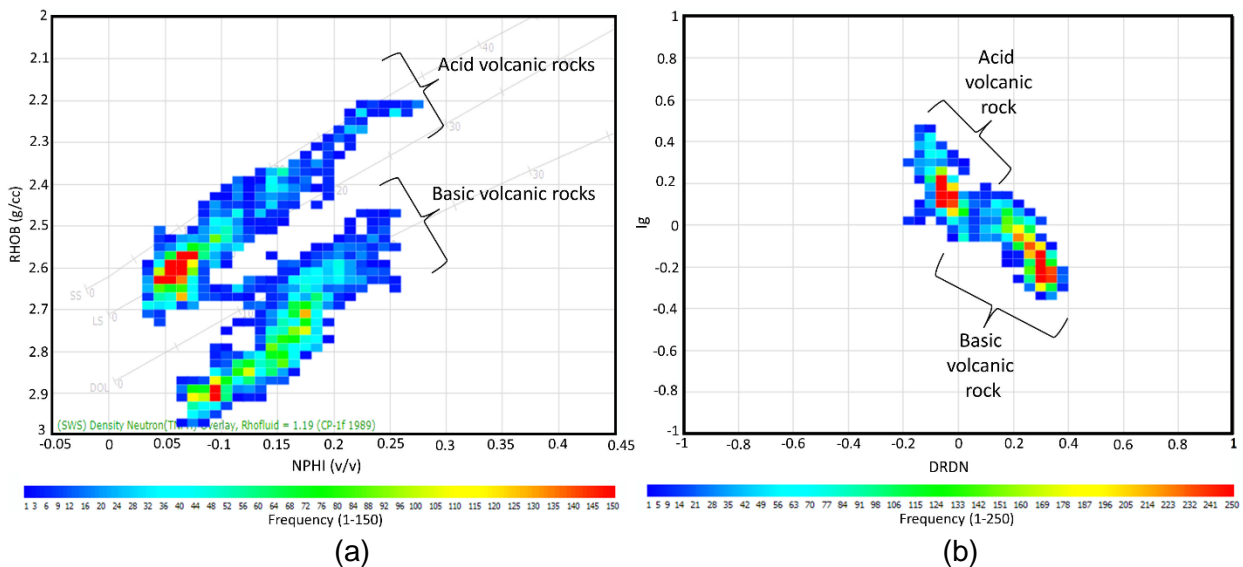
Figure 12: Two wells with the presence of acid volcanics: a) Well 7-LL-15D-RJS showing an intercalation of basalts (red in track 3) and rhyolites (orange in track 3) below a carbonate section (white in track 3); b). Well 3-BRSA-755A-RJS showing an intercalation of acidic lava flows with compositional variation from rhyolite (orange in track 3) to dacite (light brown in track 3) below a carbonate section (white in track 3).

gamma ray values and a neutron log less than or equal to zero and is always quite homogeneous in its well log characteristics (Figure 7a). Cuttings are also quite conclusive in distinguishing both lithologies, which can be obtained during well drilling or by the sample descriptions, where the anhydrite is white and recrystallized with an acicular shape when heated with HCl solution (De Oliveira et al., 2018).

Carbonates that have undergone contact metamorphism are also a false positive but, as we saw in the topic Results (Figure 6b), are easily detected by other well logs and can still be used to distinguish intrusive from extrusive basic igneous rocks. Other lithologies with very low or no porosity and high bulk densities can provide a crossover in the Igneability feature as well, such as dolomites, crystalline limestones (Figure 7a) and some metamorphic rocks.

Breakout zones in the well, usually detected by the caliper log, can also show a crossover, because the PEF reading can be affected by the drilling fluid, which is rich in barite (PE = 267 b/e). In these zones we observe an increase in PEF, but there is usually a reduction in RHOB, as can be seen in Figure 7b.

False negatives in extrusive igneous rocks

The basaltic flows have brecciated, vesiculated or altered facies (Macdonald, 1953; Walker, 1971; Self et al., 1998; Duraiswami et al., 2003, 2008; Watton et al., 2013, 2014; Duraiswami et al., 2014) that may not show the characteristic crossover of the Igneability feature (Figure 8), thus being a false negative for the method (Table 2). In subaqueous effusions, the problem is related to hyaloclastites (Figure 8a) that, while in subaerial lava flows, are related to high vesiculated or compound pahoehoe facies and brecciated rubbly pahoehoe or a'a facies (Figures 8b and 8c).

The hyaloclastites is composed of volcanic glass and igneous fragments and this glass content undergoes alteration due to interaction with water, forming hydrated minerals such as smectite, illite and zeolite (Watton et al., 2013, 2014). When the hyaloclastite has many fragments of volcanics, it shows higher density (Watton et al., 2014), and then it also exhibits a crossover in the Igneability feature. On the other hand, when volcanic glass predominates in the hyaloclastite composition, clay minerals are more abundant and may not show the crossover.

The vesiculated facies in compound pahoehoe or sheet pahoehoe lavas can be a false negative (Figures 8b and 8c) when the vesiculation is very dense, which usually occurs closer to the top of a sheet pahoehoe and along the entire compound pahoehoe succession. The brecciated facies also lack crossover, due to abrupt density variation and the common presence of clay minerals from the volcanic glass alteration present in these facies (Duraiswami et al., 2003, 2008, 2014).

The acid igneous rocks studied do not present the Igneability feature crossover (Figure 12) due to the presence of lower density minerals, such as quartz, alkali feldspars and sodium plagioclase (Table 2). This composition causes a reduction in RHOB and PEF values, preventing a crossover even though these igneous rocks are massive. In addition, commonly extrusive acid rocks are deposited as pyroclastics (or without genetic connotation, volcanoclastic rocks) because of the high

degree of explosiveness due to their high viscosity (Gill, 2010), which affects the bulk density signature. However, acid rocks can be identified due to the very high Th and K content (Ran et al., 2014), providing GR values unusually higher than the sedimentary rock (Figure 12).

Identification of the basic volcanic rock and facies using the Igneability feature

In the present work it was discussed interpretations and methods to identify the different igneous rocks commonly present in petroleum wells of the Brazilian basins, with the help of other data, such as SWC samples and image logs. It was possible to verify a response pattern of the basic well logs and the Igneous feature for these variations, which will be discussed in this topic.

Some basic igneous rocks present themselves as false negatives when we use the Igneability feature to characterize them. This occurs in zones with the presence of breccias or vesicles, always confirmed by the SWC samples and acoustic and resistive imaging logs.

Relationship of the presence of volcanic glass to false negatives

Breccias, when formed from the contact of lava with water, are called hyaloclastites, which are enriched in volcanic glass, palagonite and clay minerals from the alteration of this volcanic glass itself (Watton et al., 2014). The more glass/clay minerals and palagonite in this rock and the fewer igneous or crystal fragments such as olivine, the greater the drop in bulk density and resistivity logs, as well as the increase in sonic log and GR, according to Watton et al. (2014). Therefore, it is possible to make a direct correlation with the reason for the Igneability feature not working in some hyaloclastites, due to the drop in bulk density that these minerals cause.

Relationship between autobreccias or presence of vesicles with false negatives

Autobreccias, related to rubbly pahoehoe or a'a morphology facies, usually contain volcanic glass, zeolites, and sediments (Duraiswami et al., 2008, 2014; Rossetti et al., 2014, 2018). For this reason, these zones usually present themselves as a false negative for the Igneability feature. This textural arrangement also favors the presence of external materials, such as clay, which decreases the bulk density of the rock.

The vesicular, or even amygdaloidal, facies also suffer the direct influence of the decreasing bulk density, as well as the resistivity (RES) and sonic (DT) logs, as cited by Nelson et al. (2015), causing the same false negative in the Igneability feature, especially in areas with more vesiculation, near the top.

Relationship between massive facies and volcanoclastic facies in acid extrusive igneous rocks

Comparing two igneous rocks of the same composition, but in different textures, one being massive and the other volcanoclastic, the volcanoclastic variation will always present lower resistivity and bulk density than the massive one (Ran et al., 2014). There is also a tendency for GR to be higher due to the accumulation of U and K according to Ran et al. (2014), since acid igneous rocks are the most likely to have volcanoclastic facies and this separation is usually most appropriate for them, although a method of distinguishing the different volcanoclastic rocks from each other is not yet known.

Diagnostic well logs and crossplots for igneous rocks

From all the results and discussions regarding the variation of features in the geophysical well logs in each type of igneous rock studied, it is possible to predict some response patterns in crossplots when comparing different lithologies in terms of their compositional and textural aspects. Therefore, some well logs or calculations from ones of them (such as DRDN and Ig) can help the preliminary interpretation of the rock.

Compositional variations

Igneous rocks show variations in GR, RHOB, NPHI and DT logs when comparing their massive facies with each other and with sedimentary rocks, as already presented in Results. Some crossplots that make this kind of comparison already exist, such as the one by Ran et al. (2014), which compares responses of acid, intermediate and basic igneous rocks as to total GR and Th (ppm) values, or the crossplots by Zou et al. (2013) that compares the same lithologies as to GR x RHOB and GR x DT relationships. However, both do not include responses from major sedimentary rocks for comparison purposes.

The well logs of RHOB, GR, NPHI and DT respond well to the compositional variation of the igneous rocks,

enabling these separations, so when comparing the Ig factor with the DRDN, it is observed that there is a good variation between rhyolite and basalt, making possible to use the same for such separation. In Figure 13a, we compare the responses of both equations, Ig and DRDN, for the igneous lithologies addressed in the work (diabase, basalt and rhyolite) and the main sedimentary lithologies (anhydrite, sandstone, shale and carbonate); thus, it was possible to specify distinct fields that allow distinguishing these lithologies, mainly the igneous rocks.

Variations between DRDN with GR and Ig with GR in crossplots also help in the individualization of these igneous rocks, as we can see in Figures 13a and 13b, indicating that controlling the variation in these well logs may be the main way to identify igneous rocks and their compositional variations.

Textural variations

Each of the volcanic igneous rocks has textural variations related to the lava morphology generated at the surface. These variations mainly affect the resistivity, sonic and bulk density logs, making the identification in a volcanic section difficult. For this reason, compositional identification should be done on the portions with the highest resistivity, as they represent the most massive rock. The other variations are textural variations caused by the presence of vesicles, amygdales or breccias.

To do this kind of identification using crossplots, it is necessary to use one log that responds well to textural variation and another one that responds better to compositional variation. Therefore, a RES x GR crossplot can give a good idea of the facies variations of each volcanic rock as shown in Figure 14.

CONCLUSIONS

The Igneability feature allows the identification of basic igneous rocks in volcano-sedimentary sections and can be used as a tool associated with other log features, such as the relationship between RHOB and NPHI and the value of GR and RES for each igneous rock.

From the response of the Igneability feature and even the calculated Igneability factor, it is possible to infer facies variations in lava flows, using the fact that vesiculated and brecciated zones tend to respond as false negatives. This helps the interpretation of the environment where the volcanic rock extruded and it is always important to work in an integrated way with
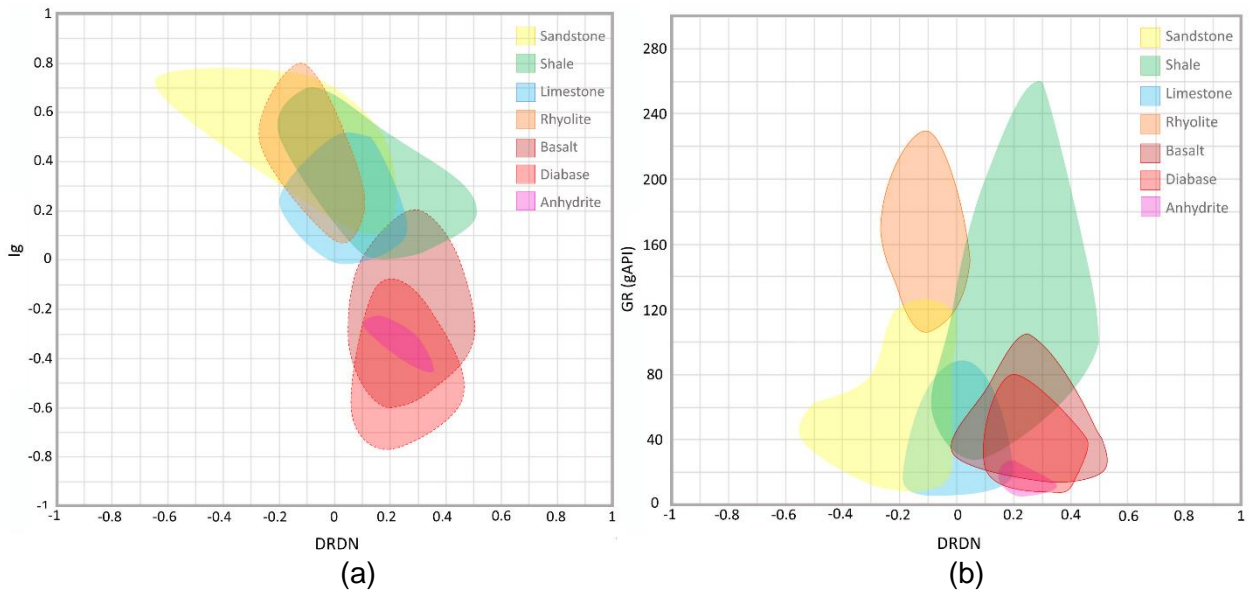
Figure 13: Crossplots indicating the variation trend of sedimentary and igneous rocks found in the studied wells: a) DRDN x Ig; b) DRDN x GR.
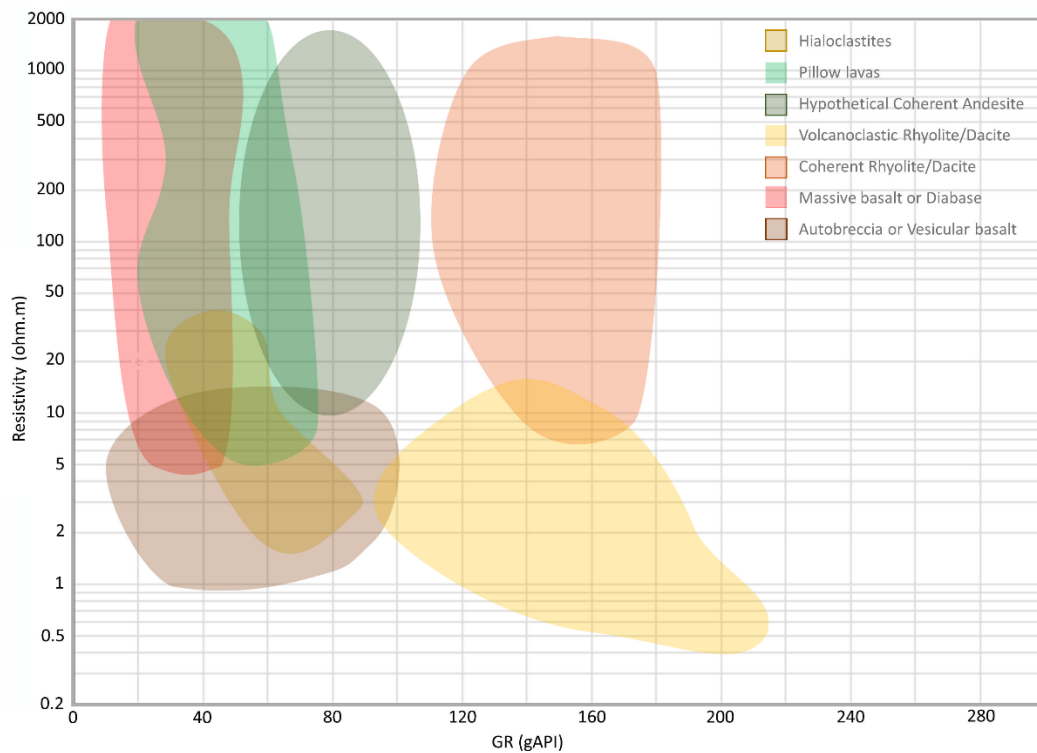

Figure 14: Crossplots between resistivity and gamma rays showing a good separation between textural and morphological variations when comparing these two well logs.

other well logs, highlighting false interpretations and understanding the compositional, faciological and alteration context of the rock.

    The GR log and the relationship between RHOB and NPHI logs (or DRDN) are used to understand in a simplified way the compositional variation of the igneous rock, suggesting whether it tends to be basic, intermediate, or acid. In this context, it is also possible

to interpret whether this rock behaves more coherent or volcanoclastic using the RES log variation, with the exception of the very vesicular facies that may behave similarly to volcanoclastic.

    For the acid igneous rocks, the Igneability feature does not work due to their mineralogical composition. However, a new feature was obtained between the relation of the GR with the Ig, enabling to individualize

the acid from the basic rocks and the sedimentary section, regardless of the morphology of the igneous rock being volcanoclastic or coherent.

From this information about igneous rocks obtained and tested with cuttings, SWC samples and image logs, it was possible to propose a response pattern for each igneous rock and its facies variations in a simplified form, therefore guiding the well interpreter during the petroleum well drilling.

REFERENCES

Bellieni, G., P. Brotzu, P. Comin-Chiaramonti, M. Ernesto, A. Melfi, I.G. Pacca, and E.M. Piccirillo, 1984, Flood basalt to rhyolite suites in the southern Parana Plateau (Brazil): palaeomagnetism, petrogenesis and geodynamic implications: Journal of Petrology, 25, 3, 579–618, doi: 10.1093/petrology/25.3.579.

Brewer, T. S., P.K. Harvey, M.A. Lovell, S. Haggas, G. Williamson, and P. Pezard, 1998, Ocean floor volcanism: constraints from the integration of core and downhole logging measurements: Geological Society, London, Special Publications, 136, 1, 341–362, doi: 10.1144/GSL.SP.1998.136.01.28.

Bücker, C.J., H. Delius, and J. Wohlenberg, 1998, Physical signature of basaltic volcanics drilled on the northeast Atlantic volcanic rifted margins: Geological Society, London, Special Publications, 136, 1, 363–374, doi: 10.1144/GSL.SP.1998.136.01.29.

De Luca, P.H.V., H. Matias, J. Carballo, D. Sineva, G. A. Pimentel, J. Tritlla, M. Esteban, R. Loma, J.L. A. Alonso, R.P. Jiménez, M. Pontet, P.B. Martinez, and V. Vega, 2017, Breaking barriers and paradigms in presalt exploration: the Pão de Açúcar discovery (offshore Brazil) in Merrill, R.K., and C.A. Sternbach, Giant fields of the decade 2000–2010: AAPG Memoir, 113, chapter 11, 177–194, doi: 10.1306/13572007M1133686.

De Miranda, F.S., A.L. Vettorazzi, P.R. da Cruz Cunha, F.B. Aragão, D. Michelon, J.L. Caldeira, E. Porsche, C. Martins, R.B. Ribeiro, A.F. Vilela, J.R. Corrêa, L.S. Silveira, and K. Andreola, 2018, Atypical igneous-sedimentary petroleum systems of the Parnaíba Basin, Brazil: seismic, well logs and cores: Geological Society, London, Special Publications, 472, 1, 341–360, doi: 10.1144/SP472.15.

De Oliveira, F.V.C.S.R.S., R.T.M. Gomes, and K.M.S. Silva, 2018, Identificação de Basaltos e Diabásios em Poços Exploratórios de Petróleo Utilizando Perfis de Densidade e Fator Fotoelétrico: 49º Congresso Brasileiro de Geologia: VII Simpósio de Vulcanismo e Ambientes Associados, Rio de Janeiro, RJ, Brazil.

De Oliveira, F.V.C.S.R.S., R.T.M. Gomes, and K.M.S. Silva, 2019, Log Features for the Characterization of Igneous Rocks in the Pre-Salt Area of Santos Basin, SE Brazil: AAPG International Conference & Exhibition. Buenos Aires, Argentina.

De Oliveira, F.V.C.S.R.S., B.M. Imbuzeiro, L.F. Ribeiro, and A.F.M. Freire, 2021, Identification of the intrusive events Mosquito and Sardinha in the Parnaíba Basin based on wireline logs, detailed description of cuttings and x-ray fluorescence analysis: 17th International Congress of the Brazilian Geophysical Society & Expogef, Rio de Janeiro, RJ, Brazil.

Dos Anjos, C.W.D., and E.M. Guimarães, 2008, Metamorfismo de contato nas rochas da Formação Irati (Permiano), norte da Bacia do Paraná: Brazilian Journal of Geology, 38, 4, 629–641, doi: 10.25249/0375-7536.2008384629641.

Duraiswami, R.A., G. Dole, and N. Bondre, 2003, Slabby pahoehoe from the western Deccan Volcanic Province: evidence for incipient pahoehoe-aa transitions: Journal of Volcanology and Geothermal Research, 121, 3–4, 195–217, doi: 10.1016/S0377-0273(02)00411-0.

Duraiswami, R.A., N.R. Bondre, and S. Managave, 2008, Morphology of rubbly pahoehoe (simple) flows from the Deccan Volcanic Province: Implications for style of emplacement: Journal of Volcanology and Geothermal Research, 177, 4, 822–836, doi: 10.1016/j.jvolgeores.2008.01.048.

Duraiswami, R.A., P. Gadpallu, T.N. Shaikh, and N. Cardin, 2014, Pahoehoe-a′a transitions in the lava flow fields of the western Deccan Traps, India-implications for emplacement dynamics, flood basalt architecture and volcanic stratigraphy: Journal of Asian Earth Sciences, 84, 146–166, doi: 10.1016/j.jseaes.2013.08.025.

Ellis, D.V., and J.M. Singer, 2007, Well logging for earth scientists: Dordrecht: Springer, 692 pp, doi: 10.1007/978-1-4020-4602-5.

Fornero, S.A., G.M. Marins, J.T. Lobo, A.F.M. Freire, and E.F. de Lima, 2019, Characterization of subaerial volcanic facies using acoustic image logs: Lithofacies and log-facies of a lava-flow deposit in the Brazilian pre-salt, deepwater of Santos Basin: Marine and Petroleum Geology, 99, 156–174, doi: 10.1016/j.marpetgeo.2018.09.029.

Freire, A.F.M., G.F.R. Santos, C.F. Silva, H.C. Pequeno, I.P.M. Leal, W.M. Lupinacci, and R. Ávila, 2019, High resolution stratigraphy using well logs to identify turbidite stages in the Massapê oil field, Recôncavo Basin, Brazil: 16th International Congress of the Brazilian Geophysical Society, Rio de Janeiro, RJ, Brazil, doi: 10.22564/16cisbgf2019.302.

Gill, R., 2010, Igneous rocks and processes: a practical guide: John Wiley & Sons, 427 pp.

Imbuzeiro, B.M., 2021, Caracterização de eletrofacies e quimiofacies em soleiras de diabásio da bacia do Parnaíba: Monografia, Universidade Federal Fluminense, Niterói, Rio de Janeiro, Brazil. 96 pp.

Jerram, D.A., 2015, Hot Rocks and Oil: Are Volcanic Margins the New Frontier?: Elsevier R&D Solutions for Oil & Gas. Geofacets, 12 pp.

Jerram, D.A., J.M. Millett, J. Kück, D. Thomas, Planke, S., E. Haskins, N. Lautze, and S. Pierdominici, 2019, Understanding volcanic facies in the subsurface: a combined core, wireline logging and image log data set from the PTA2 and KMA1 boreholes, Big Island, Hawaii: Scientific Drilling, 25, 15–33, doi: 10.5194/sd-25-15-2019.

LaFemina, P.C., 2015, Plate tectonics and volcanism, in Sigurdsson, H., The Encyclopedia of Volcanoes: Academic Press, 2nd ed., chapter 3, p. 65–92, doi: 10.1016/B978-0-12-385938-9.00003-1.

Le Maitre, R.W., A. Streckeisen, B. Zanettin, M.J. Le Bas, B. Bonin, P. Bateman, G. Bellieni, A. Dudek, S. Efremova, J. Keller, J. Lameyre, P.A. Sabine, R. Schmid, H. Sørensen, and A.R. Woolley, 2002, Igneous rocks. A Classification and Glossary of Terms: Recommendations of the International Union of Geological Sciences Subcommission on the Systematics of Igneous Rocks, 2nd ed., 236 pp. Cambridge, England: Cambridge University Press.

Lima, E.F.D., R.P. Philipp, G.C. Rizzon, B.L. Waichel, and L.D.M.M. Rossetti, 2012, Sucessões vulcânicas, modelo de alimentação e geração de domos de lava ácidos da Formação Serra Geral na região de São Marcos-Antônio Prado (RS). Geologia USP. Série Científica, São Paulo, SP, Brazil, 12, 2, p. 49–64, doi: 10.5327/Z1519-874X2012000200004.

Macdonald, G.A., 1953, Pahoehoe, aa, and block lava: American Journal of Science, 251, 3, 169–191, doi: 10.2475/ajs.251.3.169.

Marsh, B.D., 2015, Magma chambers, in Sigurdsson, H., The Encyclopedia of Volcanoes: Academic Press, 2nd ed., chapter 8, p. 185–201, doi: 10.1016/B978-0-12-385938-9.00008-0.

Millward, D., S.R. Young, B. Beddoe-Stephens, E.R. Phillips, and C.J. Evans, 2002, Gamma-ray, Spectral Gamma-ray, and Neutron-density Logs for Interpretation of Ordovician Volcanic Rocks, West Cumbria, England in Lovell M., and N. Parkinson, Eds., Geological Applications of Well Logs: AAPG Methods in Exploration Series, No. 13, Chapter 18, doi: 10.1306/Mth13780C18.

Mizusaki, A.M.P., R. Petrini, P. Bellieni, P. Comin-Chiaramonti, J. Dias, De Min, A., and E.M.

Piccirillo, 1992, Basalt magmatism along the passive continental margin of SE Brazil (Campos Basin). Contributions to Mineralogy and Petrology, 111, 2, 143–160, doi: 10.1007/BF00348948.

Nelson, C.E., D.A. Jerram, and R.W. Hobbs, 2009, Flood basalt facies from borehole data: implications for prospectivity and volcanology in volcanic rifted margins. Petroleum Geoscience, 15, 4, 313–324, doi: 10.1144/1354-079309-842.

Nelson, C.E., D.A. Jerram, J.A. Clayburn, A.M. Halton, and J. Roberge, 2015, Eocene volcanism in offshore southern Baffin Bay: Marine and Petroleum Geology, 67, 678–691, doi: 10.1016/j.marpetgeo.2015.06.002.

Pasqualon, N.G., E.F. de Lima, C.M. dos Santos Scherer, L.D.M.M. Rossetti, and F.R. da Luz, 2019, Lithofacies association and stratigraphy of the Paredão Volcano, Trindade Island, Brazil: Journal of Volcanology and Geothermal Research, 380, 48–63, doi: 10.1016/j.jvolgeores.2019.05.011.

Peate, D.W., C.J. Hawkesworth, and M.S. Mantovani, 1992, Chemical stratigraphy of the Paraná lavas (South America): classification of magma types and their spatial distribution: Bulletin of Volcanology, 55, 1, 119–139, doi: 10.1007/BF00301125.

Penna, R., S. Araújo, A. Geisslinger, R. Sansonowski, L. Oliveira, J. Rosseto, and M. Matos, 2019, Carbonate and igneous rock characterization through reprocessing, FWI imaging, and elastic inversion of a legacy seismic data set in Brazilian presalt province: The Leading Edge, 38, 1, 11–19, doi: 10.1190/tle38010011.1.

Pires, G.L.C., and E.M. Bongiolo, 2016, The nephelinitic-phonolitic volcanism of the Trindade Island (South Atlantic Ocean): Review of the stratigraphy, and inferences on the volcanic styles and sources of nephelinites: Journal of South American Earth Sciences, 72, 49–62, doi: 10.1016/j.jsames.2016.07.008

Planke, S., 1994, Geophysical response of flood basalts from analysis of wire line logs: Ocean Drilling Program Site 642, Vøring volcanic margin: Journal of Geophysical Research: Solid Earth, 99, B5, 9279-9296, doi: 10.1029/94JB00496.

Planke, S., T. Rasmussen, S.S. Rey, R. and Myklebust, 2005, Seismic characteristics and distribution of volcanic intrusions and hydrothermal vent complexes in the Vøring and Møre basins: Petroleum Geology Conference Series, Geological Society, London, 6, 1, 833–844, doi: 10.1144/0060833.

Ran, Q., Y. Wang, Y. Sun, L. Yan, and M. Tong, 2014, Lithological Identification and Prediction of

Volcanic Rock, *in* Volcanic gas reservoir characterization: Gulf Professional Publishing, Elsevier, chapter 5, 163–201, doi: 10.1016/B978-0-12-417131-2.00005-3

Riccomini, C., L.G. Sant'Anna, and C.C.G. Tassinari, 2012, Pré-sal: geologia e exploração: Revista USP, 95, 33–42, doi: 10.11606/issn.2316-9036.v0i95p33-42.

Rossetti, L.M., E.F. Lima, B.L. Waichel, C.M. Scherer, and C.J. Barreto, 2014, Stratigraphical framework of basaltic lavas in Torres Syncline main valley, southern Parana-Etendeka Volcanic Province: Journal of South American Earth Sciences, 56, 409–421, doi: 10.1016/j.jsames.2014.09.025

Rossetti, L., E.F. Lima, B.L. Waichel, M.J. Hole, M.S. Simões, and C.M. Scherer, 2018, Lithostratigraphy and volcanology of the Serra Geral Group, Paraná-Etendeka Igneous Province in southern Brazil: Towards a formal stratigraphical framework: Journal of Volcanology and Geothermal Research, 355, 98–114, doi: 10.1016/j.jvolgeores.2017.05.008

Scherer, C.M.S., 2000, Eolian dunes of the Botucatu Formation (Cretaceous) in southernmost Brazil: morphology and origin: Sedimentary Geology, 137, 1–2, 63–84, doi: 10.1016/S0037-0738(00)00135-4

Scherer, C. M., and K. Goldberg, 2007, Palaeowind patterns during the latest Jurassic–earliest Cretaceous in Gondwana: Evidence from aeolian cross-strata of the Botucatu Formation, Brazil: Palaeogeography, Palaeoclimatology, Palaeoecology, 250, 1–4, 89–100, doi: 10.1016/j.palaeo.2007.02.018

Scherer, C.M., and E.L. Lavina, 2006, Stratigraphic evolution of a fluvial-eolian succession: the example of the Upper Jurassic – Lower Cretaceous Guará and Botucatu formations, Paraná Basin, Southernmost Brazil: Gondwana Research, 9, 4, 475–484, doi: 10.1016/j.gr.2005.12.002

Self, S., L. Keszthelyi, and T. Thordarson, 1998, The importance of pahoehoe: Annual Review of Earth and Planetary Sciences, 26, 1, 81–110, doi: 10.1146/annurev.earth.26.1.81

Spacapan, J.B., O. Palma, O. Galland, K. Senger, R. Ruiz, R. Manceda, and H.A. Leanza, 2020, Low resistivity zones at contacts of igneous intrusions emplaced in organic-rich formations and their implications on fluid flow and petroleum systems:

A case study in the northern Neuquén Basin, Argentina: Basin Research, 32, 1, 3–24, doi: 10.1111/bre.12363.

Thomaz Filho, A., A.M.P. Mizusaki, and L. Antonioli, 2008, Magmatismo nas bacias sedimentares brasileiras e sua influência na geologia do petróleo: Revista Brasileira de Geociências, 38, Suppl. 2, 128–137, doi: 10.25249/0375-7536.2008382S128137.

Umino, S., 2012, Emplacement mechanism of off-axis large submarine lava field from the Oman Ophiolite: Journal of Geophysical Research: Solid Earth, 117, B11, doi: 10.1029/2012JB009198

Waichel, B.L., E.F. de Lima, A.R. Viana, C.M. Scherer, G.V. Bueno, and G. Dutra, 2012, Stratigraphy and volcanic facies architecture of the Torres Syncline, Southern Brazil, and its role in understanding the Paraná-Etendeka Continental Flood Basalt Province: Journal of Volcanology and Geothermal Research, 215, 74–82, doi: 10.1016/j.jvolgeores.2011.12.004.

Walker, G.P.L., 1971, Compound and simple lava flows and flood basalts: Bulletin Volcanologique, 35, 3, 579–590, doi: 10.1007/BF02596829

Watton, T.J., D.A. Jerram, T. Thordarson, and R.J. Davies, 2013, Three-dimensional lithofacies variations in hyaloclastite deposits: Journal of Volcanology and Geothermal Research, 250, 19–33, doi: 10.1016/j.jvolgeores.2012.10.011.

Watton, T.J., K.A. Wright, D.A. Jerram, and R.J. Brown, 2014, The petrophysical and petrographical properties of hyaloclastite deposits: Implications for petroleum exploration. AAPG Bulletin, 98, 3, 449–463, doi: 10.1306/08141313029.

White, J.D., J. McPhie, and S.A. Soule, 2015, Submarine lavas and hyaloclastite in Sigurdsson, H., The encyclopedia of volcanoes: Academic Press, 2nd ed., pp. 363–375, doi: 10.1016/B978-0-12-385938-9.00019-5.

Winter, W.R., R.J. Jahnert, and A.B. França, 2007, Bacia de Campos: Boletim de Geociências da PETROBRAS, 15, 2, 511–529.

Zou, C.N., Z. Yang, S.Z. Tao, X.J. Yuan, R.K. Zhu, L.H. Hou, S.T. Wu, L. Sun, G.S. Zhang, B. Bai, L. Wang, X.H. Gao, and Z.L. Pang, 2013, Continuous hydrocarbon accumulation over a large area as a distinguishing characteristic of unconventional petroleum: The Ordos Basin, North-Central China: Earth-Science Reviews, 126, 358–369, doi: 10.1016/j.earscirev.2013.08.006.